Mon. Not. R. Astron. Soc. **309**, 447–460 (1999)

Rates of tidal disruption of stars by massive central black holes

John Magorrian[1,2] and Scott Tremaine[3]
[1]*CITA, University of Toronto, 60 St George Street, Toronto, Ontario, Canada M5S 3H8*
[2]*Institute of Astronomy, Madingley Road, Cambridge CB3 0HA*
[3]*Princeton University Observatory, Peyton Hall, Princeton, NJ 08544, USA*

Accepted 1999 June 1. Received 1999 May 20; in original form 1999 February 1

ABSTRACT

There is strong evidence for some kind of massive dark object in the centres of many galaxy bulges. The detection of flares from tidally disrupted stars could confirm that these objects are black holes (BHs). Here we present calculations of the stellar disruption rates in detailed dynamical models of real galaxies, taking into account the refilling of the loss cone of stars on disruptable orbits by two-body relaxation and tidal forces in non-spherical galaxies. The highest disruption rates (one star per 10^4 yr) occur in faint ($L \lesssim 10^{10}\,L_\odot$) galaxies, which have steep central density cusps. More luminous galaxies are less dense and have much longer relaxation times and more massive BHs. Dwarf stars in such galaxies are swallowed whole by the BH and hence do not emit flares; giant stars could produce flares as often as every 10^5 yr, although the rate depends sensitively on the shape of the stellar distribution function. We discuss the possibility of detecting disruption flares in current supernova searches. The total mass of stars consumed over the lifetime of the galaxy is of the order of $10^6\,M_\odot$, independent of galaxy luminosity; thus, disrupted stars may contribute significantly to the present BH mass in galaxies fainter than $\sim 10^9\,L_\odot$.

Key words: celestial mechanics, stellar dynamics – galaxies: kinematics and dynamics – galaxies: nuclei.

1 INTRODUCTION

Both gas- and stellar-dynamical measurements indicate that many, if not most, galaxies harbour some kind of massive central dark object (MDO) (e.g. Kormendy & Richstone 1995; Magorrian et al. 1998; van der Marel 1998; Ford et al. 1998; Ho 1998). Indirect arguments suggest that these MDOs are most probably black holes (BHs) because dark clusters of the required mass and size are difficult to construct and maintain (Maoz 1998), and because dead quasar engines (Lynden-Bell 1969) should lurk in the centres of many nearby galaxies (Sołtan 1982; Chokshi & Turner 1992). An inevitable source of fuel for these dead quasars is the debris from tidal disruption of stars on almost radial orbits. Much of the debris from a disrupted star gets ejected, but a portion remains bound to the BH and emits a 'flare' lasting a few months to a year (Rees 1988, 1998; Lee 1999). The spectrum is expected to be mainly thermal, peaking at extreme UV or soft X-ray wavelengths. Plausible models (Ulmer 1999) predict *V*-band luminosities of $\sim 10^9\,L_\odot$, and even higher luminosities in the *U* band (but see also Ulmer, Paczyński & Goodman 1998). Such flares ought to be easily detectable, but as yet there is only marginal observational evidence that they occur (Renzini et al. 1995; Komossa & Bade 1999).

Recently, Magorrian et al. (1998, hereafter Paper I) used *Hubble Space Telescope* (*HST*) photometry and ground-based kinematics to constrain MDO masses for a sample of 32 nearby galaxies, assuming that each is well described by a two-integral axisymmetric model. The purpose of the present paper is to calculate the tidal disruption rates for these two-integral models, assuming that their MDOs are BHs. The paper is organized as follows. The following section gives a brief description of our modelling assumptions and describes the 'loss cone' of stars on disruptable orbits. In Section 3 we calculate the steady-state disruption rate owing to the diffusion into the loss cone of stars on centrophobic loop orbits. Similar calculations of this rate have recently been presented by Syer & Ulmer (1999). In addition, in a flattened or triaxial galaxy, a significant portion of phase space is occupied by centrophilic orbits. We investigate the effect these have on the disruption rate in Section 4. We then use these results to estimate the effects of consumed stars on BH masses (Section 5) and to estimate the expected rate of detection of flares in surveys (Section 6). Before summing up, we discuss possible shortcomings of our models in Section 7.

2 GENERAL BACKGROUND: THE LOSS CONE

Consider a galaxy with a central BH of mass $M_\bullet$. Let us suppose for simplicity that the galaxy is otherwise composed entirely of

stars of mass m_* and radius r_*. (The generalization to a range of m_* and r_* is dealt with in Appendix A.) Then, neglecting relativistic effects, a star that comes within a distance

$$r_{\rm t} = \left(\eta^2 \frac{M_\bullet}{m_*}\right)^{1/3} r_* \tag{1}$$

of the central BH will be tidally disrupted, where $\eta \simeq 2.21$ for a homogeneous, incompressible body and 0.844 for an $n = 3$ polytrope (Sridhar & Tremaine 1992; Diener et al. 1995). We define the 'loss cone' to consist of all orbits with pericentres less than $r_{\rm t}$. Of course, if $r_{\rm t} \lesssim r_{\rm S} \equiv 2GM_\bullet/c^2$ the star is swallowed whole by the BH, without producing a flare. Thus for $M_\bullet \gtrsim 10^8\,{\rm M}_\odot$ solar-type stars are swallowed whole and only giants are disrupted outside the horizon of the BH. However, it often proves convenient to ignore the fact that the BH has a horizon so that results obtained for some particular values of r_* and m_* can be scaled for other values. Thus in what follows, our 'consumption' rates are the rates at which stars come within a radius $r_{\rm t}$ of the BH, even if this lies inside the horizon of the BH. In contrast we shall use the term 'flaring' rate to refer to the rate of disruption of stars outside the horizon of the BH.

Let us first examine the loss cone in a spherical galaxy. The distribution function (DF) $f(\boldsymbol{x},\boldsymbol{v})$ is defined such that $f(\boldsymbol{x},\boldsymbol{v})\,{\rm d}^3\boldsymbol{x}\,{\rm d}^3\boldsymbol{v}$ is the probability of finding a star within a volume ${\rm d}^3\boldsymbol{x}\,{\rm d}^3\boldsymbol{v}$ of $(\boldsymbol{x},\boldsymbol{v})$. By Jeans' theorem, the DF of a spherical galaxy depends on $(\boldsymbol{x},\boldsymbol{v})$ only through the orbital binding energy per unit mass $\mathscr{E} = \psi(\boldsymbol{x}) - \frac{1}{2}v^2$ and angular momentum per unit mass $J = |\boldsymbol{x}\times\boldsymbol{v}|$ of the stars, where the relative gravitational potential $\psi(r)$ is related to the potential of the galaxy $\Phi(r)$ through $\psi(r) \equiv -\Phi(r)$. In terms of $(\mathscr{E},J)$ the loss cone is given by

$$J^2 \leqslant J_{\rm lc}^2(\mathscr{E}) \equiv 2r_{\rm t}^2[\psi(r_{\rm t}) - \mathscr{E}] \simeq 2GM_\bullet r_{\rm t}, \tag{2}$$

and we have assumed $\mathscr{E} \ll GM_\bullet/r_{\rm t}$ (i.e. most stars are consumed from nearly radial orbits). The number of stars in any small volume of phase space ${\rm d}\mathscr{E}\,{\rm d}J^2$ around $(\mathscr{E},J^2)$ is

$$\begin{aligned} N(\mathscr{E},J^2)\,{\rm d}\mathscr{E}\,{\rm d}J^2 &= \int {\rm d}^3\boldsymbol{x}\,{\rm d}^3\boldsymbol{v} f(\mathscr{E},J^2) \\ &= 4\pi^2 f(\mathscr{E},J^2)P(\mathscr{E},J^2)\,{\rm d}\mathscr{E}\,{\rm d}J^2, \end{aligned} \tag{3}$$

where $P(\mathscr{E},J^2)$ is the radial period of an orbit with energy $\mathscr{E}$ and angular momentum J. For almost radial loss-cone orbits we may approximate $P(\mathscr{E},J^2)$ by $P(\mathscr{E}) \equiv P(\mathscr{E},0)$. So, for a spherical galaxy with isotropic DF $f(\mathscr{E})$, the number of stars $N_{\rm lc}(\mathscr{E})$ in the (full) loss cone per unit energy is given by

$$N_{\rm lc}(\mathscr{E})\,{\rm d}\mathscr{E} = 4\pi^2 f(\mathscr{E})P(\mathscr{E})J_{\rm lc}^2(\mathscr{E})\,{\rm d}\mathscr{E}, \tag{4}$$

while the total number of stars $N(\mathscr{E})$ per unit energy interval is given by

$$N(\mathscr{E})\,{\rm d}\mathscr{E} = 4\pi^2 f(\mathscr{E})\,{\rm d}\mathscr{E}\int_0^{J_{\rm c}^2(\mathscr{E})} P(\mathscr{E},J^2)\,{\rm d}J^2, \tag{5}$$

where $J_{\rm c}(\mathscr{E})$ is the angular momentum of a circular orbit of energy $\mathscr{E}$.

In an axisymmetric galaxy with an integrable potential, the DF is a function $f(\mathscr{E},J_z,J_3)$, where J_z is the component of angular momentum along the symmetry (z-)axis and J_3 is a third integral. Numerical experiments show that we may reasonably make the approximation $J_3 \simeq J$ (e.g. Binney & Tremaine 1987). Then the number of stars in any small volume of phase space ${\rm d}\mathscr{E}\,{\rm d}J_z\,{\rm d}J$ is just

$$N(\mathscr{E},J_z,J)\,{\rm d}\mathscr{E}\,{\rm d}J_z\,{\rm d}J = 4\pi^2 f(\mathscr{E},J_z,J)P(\mathscr{E},J_z,J)\,{\rm d}\mathscr{E}\,{\rm d}J_z\,{\rm d}J. \tag{6}$$

If P and f are approximately independent of J_z we can integrate over J_z from $-J$ to J and recover equation (3). Therefore, the expressions (4) and (5) given above also apply to axisymmetric galaxies, at least for the interesting low-J orbits. In particular, two-integral axisymmetric models correspond to spherical isotropic models if we replace $f(\mathscr{E})$ by $f(\mathscr{E},J_z=0)$. In what follows, we write $f(\mathscr{E})$ for the axisymmetric DF $f(\mathscr{E},J_z=0)$, $f(\mathscr{E},J^2)$ for $f(\mathscr{E},J_z=0,J^2)$ etc.

For each of the two-integral models of Paper I it is straightforward to use the axisymmetric luminosity distribution $j(R,z)$ and best-fitting BH mass $M_\bullet$ and stellar mass-to-light ratio Υ to obtain $f(\mathscr{E})$, $N(\mathscr{E})$ and $N_{\rm lc}(\mathscr{E})$. The method is as follows. The best-fitting stellar mass density to the observations is $\rho(R,z) = \Upsilon j(R,z)$. Assuming all stars are of mass m_*, the corresponding number density $\nu(R,z) = \Upsilon j(R,z)/m_*$. The $J_z = 0$ slice of the DF then follows on inverting

$$\nu(0,z) = 4\pi\int_0^{\psi(0,z)} f(\mathscr{E},J_z=0)\sqrt{2[\psi(0,z)-\mathscr{E}]}\,{\rm d}\mathscr{E}. \tag{7}$$

We solve equation (7) for $f(\mathscr{E},J_z=0)$ using the numerical method described in Appendix C.

Fig. 1 shows the resulting $f(\mathscr{E})$, $N(\mathscr{E})$ and $N_{\rm lc}(\mathscr{E})$ for the edge-on model of M32, assuming that it is composed entirely of solar-type stars. Both $f(\mathscr{E})$ and $N_{\rm lc}(\mathscr{E})$ peak at $\mathscr{E} \sim \mathscr{E}_{\rm h} \equiv \psi(r_{\rm h})$, where $r_{\rm h}$ is the radius of the sphere of influence of the BH, defined in terms of the intrinsic velocity dispersion of the galaxy $\sigma(r)$ through

$$\sigma^2(r_{\rm h}) = \frac{GM_\bullet}{r_{\rm h}} \equiv \sigma_{\rm h}^2. \tag{8}$$

The results depend on the assumed inclination angle of the galaxy, because flatter galaxies have fewer stars on low-angular-momentum orbits. For this edge-on model, the full loss cone contains about $15\,{\rm M}_\odot$ of stars, approximately half of which are

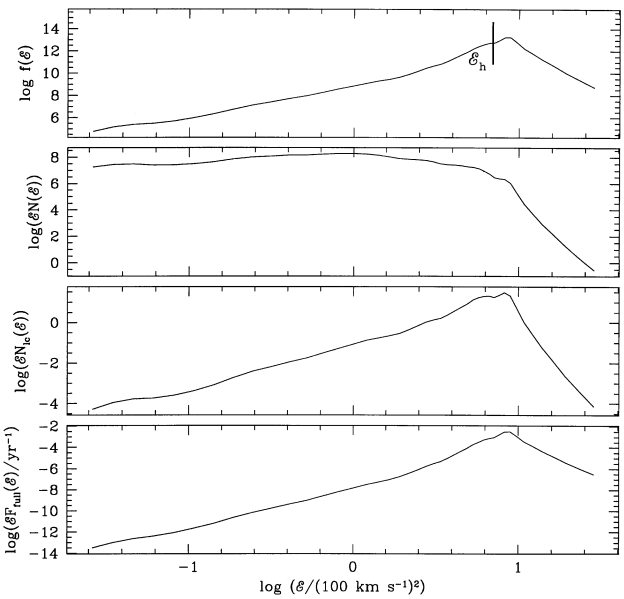

Figure 1. Full loss cone in the edge-on model of M32. The top panel shows the isotropic DF $f(\mathscr{E})$ obtained assuming the galaxy is composed of solar-type stars. The others show $N(\mathscr{E})$ and $N_{\rm lc}(\mathscr{E})$ given by equations (4) and (5), and the consumption rate were the loss cone full, $F_{\rm full} = N_{\rm lc}(\mathscr{E})/P(\mathscr{E})$. The heavy vertical line marks the energy $\mathscr{E}_{\rm h} = \psi(r_{\rm h})$, where $r_{\rm h}$ is the radius of the sphere of influence of the BH (equation 8).

bound to the BH. Full loss cones in larger, core galaxies contain up to about $2000\,\mathrm{M}_\odot$.

The shapes of $f(\mathscr{E})$, $N_{\rm lc}(\mathscr{E})$ and $N(\mathscr{E})$ for $\mathscr{E} \gtrsim \mathscr{E}_{\rm h}$ can be understood as follows. For $r \ll r_{\rm h}$, $\psi = GM_\bullet/r$, $J_{\rm c}^2(\mathscr{E}) = G^2M_\bullet^2/2\mathscr{E}$, and $P(\mathscr{E}) = 2\pi GM_\bullet/(2\mathscr{E})^{3/2}$. If the number density of stars is $\nu(r) = \nu_0(r_{\rm h}/r)^\alpha$ then

$$f(\mathscr{E}) = (2\pi\sigma_{\rm h}^2)^{-\frac{3}{2}}\nu_0\frac{\Gamma(\alpha+1)}{\Gamma\left(\alpha-\frac{1}{2}\right)}\left(\frac{\mathscr{E}}{\sigma_{\rm h}^2}\right)^{\alpha-\frac{3}{2}}, \quad \frac{1}{2} < \alpha < 3. \tag{9}$$

Equations (4) and (5) then give for $\mathscr{E} \gtrsim \mathscr{E}_{\rm h}$

$$N(\mathscr{E}) \simeq \frac{10^4}{(100\,\mathrm{km\,s^{-1}})^2}\left(\frac{M_\bullet}{10^6\,\mathrm{M}_\odot}\right)^3\left(\frac{\nu_0}{10^5\,\mathrm{pc^{-3}}}\right) \times \left(\frac{100\,\mathrm{km\,s^{-1}}}{\sigma_{\rm h}}\right)^8\left(\frac{\mathscr{E}}{\sigma_{\rm h}^2}\right)^{\alpha-4}$$

$$N_{\rm lc}(\mathscr{E}) \simeq \frac{0.5}{(100\,\mathrm{km\,s^{-1}})^2}\left(\frac{M_\bullet}{10^6\,\mathrm{M}_\odot}\right)^{7/3}\left(\frac{\nu_0}{10^5\,\mathrm{pc^{-3}}}\right) \times \left(\frac{100\,\mathrm{km\,s^{-1}}}{\sigma_{\rm h}}\right)^6\left(\frac{\mathscr{E}}{\sigma_{\rm h}^2}\right)^{\alpha-3}\left(\frac{r_*}{\mathrm{r}_\odot}\right)\left(\frac{m_\odot}{m_*}\right)^{1/3}, \tag{10}$$

both steeply falling functions of $\mathscr{E}$. Thus $N(\mathscr{E})$ and $N_{\rm lc}(\mathscr{E})$ decline at large $\mathscr{E}$, and $f(\mathscr{E})$ declines if and only if $\alpha < 3/2$. For energies $\mathscr{E} \lesssim \mathscr{E}_{\rm h}$ (radii $r \gtrsim r_{\rm h}$), the potential becomes a much shallower function of radius, and so both $f(\mathscr{E})$ and $N_{\rm lc}(\mathscr{E})$ fall as $\mathscr{E}$ is reduced from $\mathscr{E} \sim \mathscr{E}_{\rm h}$, whereas $N(\mathscr{E})$ continues to rise owing to its dependence on $J_{\rm c}^2$. Thus $N_{\rm lc}(\mathscr{E})$ always peaks near $\mathscr{E}_{\rm h}$, and $f(\mathscr{E})$ peaks near $\mathscr{E}_{\rm h}$ in core galaxies. [M32 is the only 'power-law' (Lauer et al. 1995) galaxy in our sample for which $f(\mathscr{E})$ declines at large $\mathscr{E}$. The reason is that the classification of M32 as a power law is based on its appearance at distances typical for our galaxy sample, whereas in fact it is much closer. The density profile of M32 is quite shallow within the innermost arcsec or so, a feature which would not be resolved if it were not so close.]

As $N_{\rm lc}(\mathscr{E})$ peaks at $\mathscr{E} \sim \mathscr{E}_{\rm h} \sim \sigma_{\rm h}^2$, the characteristic time-scale for emptying a full loss cone is

$$P(\mathscr{E}_{\rm h}) \sim 10^4\left(\frac{M_\bullet}{10^6\,\mathrm{M}_\odot}\right)\left(\frac{100\,\mathrm{km\,s^{-1}}}{\sigma_{\rm h}}\right)^3\,\mathrm{yr}. \tag{11}$$

The flux of stars per unit energy into the maw of the BH when the loss cone is full is just $F^{\rm full}(\mathscr{E}) = N_{\rm lc}(\mathscr{E})/P(\mathscr{E})$. For $\mathscr{E} \gtrsim \mathscr{E}_{\rm h}$,

$$F^{\rm full}(\mathscr{E}) \simeq \frac{4\times10^{-5}\,\mathrm{yr^{-1}}}{(100\,\mathrm{km\,s^{-1}})^2}\left(\frac{M_\bullet}{10^6\,\mathrm{M}_\odot}\right)^{4/3}\left(\frac{\nu_0}{10^5\,\mathrm{pc^{-3}}}\right) \times \left(\frac{100\,\mathrm{km\,s^{-1}}}{\sigma_{\rm h}}\right)^3\left(\frac{\mathscr{E}}{\sigma_{\rm h}^2}\right)^{\alpha-\frac{3}{2}}\left(\frac{r_*}{\mathrm{r}_\odot}\right)\left(\frac{\mathrm{m}_\odot}{m_*}\right)^{1/3}. \tag{12}$$

Integrating over $\mathscr{E}$, this reduces to the expression given by Rees (1988) when $\alpha = 0$. For $\alpha > \frac{1}{2}$ the total rate $\int F^{\rm full}(\mathscr{E})\,\mathrm{d}\mathscr{E}$ diverges, being dominated by the consumption of the most tightly bound stars.

3 REPOPULATING THE LOSS CONE BY TWO-BODY RELAXATION

Two-body relaxation causes stars to diffuse gradually into a depleted loss cone. Stars diffuse in both $\mathscr{E}$ and J^2 with the same characteristic time-scale $t_{\rm relax}$, but diffusion in J^2 is the dominant contributor to the consumption rate: for all but the most tightly bound stars [of which there are very few – see equation (10)], the loss-cone boundary is almost independent of $\mathscr{E}$ (equation 2). Not all stars that enter the loss cone are consumed: if the characteristic change in J^2 per orbit $\Delta J^2 \sim J_{\rm c}^2(\mathscr{E})P(\mathscr{E})/t_{\rm relax}(\mathscr{E}) \gg J_{\rm lc}^2(\mathscr{E})$, stars with $r \gg r_{\rm t}$ can wander in and out of the loss cone many times per orbit with impunity (Lightman & Shapiro 1977).

In this section we calculate the steady-state rate of diffusion of stars into the loss cone. Our calculation is a simple generalization of Cohn & Kulsrud (1978, hereafter CK) to non-Keplerian potentials. Let us define $f(\mathscr{E}, J^2; r)\,\mathrm{d}\mathscr{E}\,\mathrm{d}J^2$ to be the probability of finding a star within $\mathrm{d}\mathscr{E}\,\mathrm{d}J^2$ of $(\mathscr{E}, J^2)$ at a given radius r. Neglecting the effects of large-angle scatterings, the evolution of $f(\mathscr{E}, J; r)$ near the loss cone can be approximated by the Fokker–Planck equation (e.g. CK)

$$\frac{\partial f}{\partial t} + v_{\rm r}\frac{\partial f}{\partial r} = \frac{\partial}{\partial R}\left[-\langle\Delta R\rangle f + \frac{1}{2}\frac{\partial}{\partial R}(\langle(\Delta R)^2\rangle f)\right], \tag{13}$$

where $R \equiv J^2/J_{\rm c}^2(\mathscr{E})$, $v_{\rm r} = [2(\psi(r) - \mathscr{E})]^{1/2}$ is the radial velocity, and the diffusion coefficients $\langle\Delta R\rangle$ and $\langle(\Delta R)^2\rangle$, both functions of $(\mathscr{E}, R; r)$, measure the rate at which two-body encounters cause stars to diffuse in R. We derive expressions for the diffusion coefficients in Appendix B, and find that $\langle\Delta R\rangle = \frac{1}{2}\partial\langle(\Delta R)^2\rangle/\partial R$, simplifying the right-hand side of equation (13). We seek a steady-state solution, so $\partial f/\partial t = 0$. Expanding the diffusion coefficients about $R = 0$, the Fokker–Planck equation for $R \ll 1$ becomes

$$\frac{\partial f}{\partial r} = \frac{\mu}{v_{\rm r}}\frac{\partial}{\partial R}\left(R\frac{\partial f}{\partial R}\right), \tag{14}$$

where $\mu(\mathscr{E}, r)$ is the limiting value of $\langle(\Delta R)^2\rangle/2R$ as $R \to 0$, which is given by $\mu = 2r^2\langle\Delta v_{\rm t}^2\rangle/J_{\rm c}^2$, where $\langle\Delta v_{\rm t}^2\rangle$ is the diffusion coefficient for tangential velocity (Appendix B). Integrating over some small volume of phase space $\mathrm{d}^3\boldsymbol{x}\,\mathrm{d}^3\boldsymbol{v} = 8\pi^2J_{\rm c}^2(\mathscr{E})\,\mathrm{d}r\,\mathrm{d}R\,\mathrm{d}\mathscr{E}/v_{\rm r}$ yields the $(-R)$-directed flux of stars with energies between $\mathscr{E}$ and $\mathscr{E} + \mathrm{d}\mathscr{E}$:

$$F^{\rm lc}(\mathscr{E})\,\mathrm{d}\mathscr{E} = 8\pi^2J_{\rm c}^2(\mathscr{E})\,\mathrm{d}\mathscr{E}\int_{r_-}^{r_+}\frac{\mathrm{d}r}{v_{\rm r}}\mu R\frac{\partial f}{\partial R}. \tag{15}$$

Here r_+ and r_- are the apocentre and pericentre radii of an orbit with energy $\mathscr{E}$ and angular momentum R.

Our solution $f(\mathscr{E}, R; r)$ of equation (14) must satisfy two conditions. First, because stars on loss-cone orbits are consumed at pericentre $r = r_-$, we must have $f(\mathscr{E}, R; r_-) = 0$ for $R < R_{\rm lc}(\mathscr{E})$. (Strictly speaking, we should impose this condition for all $r < r_{\rm t}$.) Secondly, because we seek a steady-state solution, $f(\mathscr{E}, R; r)$ should not change from one orbital period to another. To accommodate the latter condition, we follow CK in changing variable from r to the time-like

$$\tau \equiv \int_{r_-}^{r}\frac{\mu\,\mathrm{d}r}{v_{\rm r}}\Big/2\int_{r_-}^{r_+}\frac{\mu\,\mathrm{d}r}{v_{\rm r}} \equiv \int_{r_-}^{r}\frac{\mu\,\mathrm{d}r}{v_{\rm r}}\Big/P(\mathscr{E})\bar{\mu}(\mathscr{E}), \tag{16}$$

so that $\tau = 0, 1, 2, \ldots$ correspond to successive pericentre passages of an imaginary star of energy $\mathscr{E}$ and angular momentum R. The variable $\bar{\mu}(\mathscr{E})$ is just the orbit-averaged diffusion coefficient. The Fokker–Planck equation then becomes

$$\frac{\partial f}{\partial \tau} = P\bar{\mu}\frac{\partial}{\partial R}\left(R\frac{\partial f}{\partial R}\right), \tag{17}$$

and our boundary conditions on $f(\mathscr{E}, R; \tau)$ are

$$f(\mathscr{E}, R; 0) = f(\mathscr{E}, R; 1)$$

$$f(\mathscr{E}, R; 0) = f(\mathscr{E}, R; 1) = 0 \qquad \text{if } R < R_{\rm lc}(\mathscr{E}). \tag{18}$$

CK point out that the orbit-averaged solution to equation (17) subject to the boundary conditions (18) is well approximated by

$$f(\mathscr{E},R) \simeq A(\mathscr{E}) \ln\left[\frac{R}{R_0(\mathscr{E})}\right], \qquad R > R_0, \tag{19}$$

where $A(\mathscr{E})$ is a constant and R_0 depends on $q(\mathscr{E}) \equiv P(\mathscr{E})\bar{\mu}(\mathscr{E})/R_{\rm lc}(\mathscr{E})$ through

$$R_0(\mathscr{E}) = R_{\rm lc}(\mathscr{E}) \times \begin{cases} \exp(-q) & \text{for } q(\mathscr{E}) > 1 \\ \exp(-0.186q - 0.824\sqrt{q}) & \text{for } q(\mathscr{E}) < 1 \end{cases}. \tag{20}$$

In the 'pinhole' limit (Lightman & Shapiro 1977) $q \gg 1$, stars can wander in and out of the loss cone many times without ill effect, and this is reflected in the fact that the DF goes to zero only at $R_0 \ll R_{\rm lc}$. On the other hand, in the 'diffusion' limit $q \ll 1$ stars cannot wander very far into the loss cone without being consumed, so R_0 is very nearly equal to $R_{\rm lc}$.

Because most stars have $R_0(\mathscr{E}) \ll 1$, the DF given by equation (19) is very close to the 'isotropized' DF

$$\bar{f}(\mathscr{E}) \equiv A(\mathscr{E}) \int_{R_0(\mathscr{E})}^{1} \ln\left(\frac{R}{R_0(\mathscr{E})}\right) {\rm d}R \simeq A(\mathscr{E}) \ln R_0^{-1}(\mathscr{E}). \tag{21}$$

So, if a galaxy is observed to be consistent with an isotropic DF $\bar{f}(\mathscr{E})$, then its underlying DF, for $R > R_0(\mathscr{E})$, is really

$$f(\mathscr{E},R) = \frac{\bar{f}(\mathscr{E})}{\ln R_0^{-1}(\mathscr{E})} \ln\left(\frac{R}{R_0(\mathscr{E})}\right). \tag{22}$$

Substituting this into equation (15) gives the rate of consumption of stars by the BH,

$$F^{\rm lc}(\mathscr{E})\,{\rm d}\mathscr{E} = 4\pi^2 P(\mathscr{E}) J_{\rm c}^2(\mathscr{E}) \bar{\mu}(\mathscr{E}) \frac{\bar{f}(\mathscr{E})\,{\rm d}\mathscr{E}}{\ln R_0^{-1}(\mathscr{E})}. \tag{23}$$

Using equation (20) we can rewrite this result as (see also equation (12) of Lightman & Shapiro 1977)

$$F^{\rm lc}(\mathscr{E})\,{\rm d}\mathscr{E} \sim \begin{cases} F^{\rm max}(\mathscr{E})\,{\rm d}\mathscr{E}/\ln(GM/4\mathscr{E}r_{\rm t}) & q \ll -\ln R_{\rm lc} \\ q^{-1} F^{\rm max}(\mathscr{E})\,{\rm d}\mathscr{E} & q \gg -\ln R_{\rm lc} \end{cases}, \tag{24}$$

where $F^{\rm max}(\mathscr{E}) \equiv 4\pi^2 P(\mathscr{E}) J_{\rm c}^2(\mathscr{E}) \bar{\mu}(\mathscr{E}) \bar{f}(\mathscr{E}) \simeq N(\mathscr{E}) \bar{\mu}(\mathscr{E})$ is an estimate of the maximum possible flux through a constant-$\mathscr{E}$ surface in phase space (Lightman & Shapiro 1977). Using the definition of q we can confirm that $F^{\rm lc}(\mathscr{E}) \simeq F^{\rm full}(\mathscr{E})$ for $q \gg -\ln R_{\rm lc}$, where $F^{\rm full}$ is the consumption rate when the loss cone is full (equation 12). Note that the transition between pinhole and diffusion régimes is at $q \simeq -\ln R_{\rm lc}$ rather than $q \simeq 1$ as simpler arguments would suggest (e.g. Lightman & Shapiro 1977).

3.1 Results

Having $\bar{f}(\mathscr{E})$ from equation (7), it is straightforward to calculate $\bar{\mu}(\mathscr{E})$ and use equation (23) to calculate the consumption rate for each of the galaxy models in Paper I. Fig. 2 shows the results for our edge-on models of M32 and M87, assuming that the stars all have solar mass and radius. Note that in both cases $F^{\rm lc}(\mathscr{E})$ peaks at $\mathscr{E} \simeq \mathscr{E}_{\rm h}$, a result which we find holds generally to within about 20 per cent: at $\mathscr{E} \simeq \mathscr{E}_{\rm h}$, $\bar{f}(\mathscr{E})$ turns over (Section 2), $\bar{\mu}(\mathscr{E})$ levels off, and the rates of change of both $J_{\rm c}(\mathscr{E})$ and $P(\mathscr{E})$ peak. Thus, while a cursory glance at equation (24) might suggest that $F^{\rm lc}(\mathscr{E})$ should peak where $q \simeq -\ln R_{\rm lc}$, it is the $F_{\rm max}(\mathscr{E})$ factor that is the dominant influence on the shape of $F^{\rm lc}(\mathscr{E})$. Indeed, stars in large galaxies like M87 just barely make it into the $q \gg 1$ pinhole régime and never have $q \gg -\ln R_{\rm lc}$.

One process that has been neglected in this local Fokker–Planck analysis is the resonant relaxation described by Rauch & Tremaine (1996) and Rauch & Ingalls (1998): orbits in the nearly Keplerian potential close to the BH can be thought of as slowly precessing ellipses, the mutual torques of which allow much faster relaxation in angular momentum. This effect can enhance the relaxation rate a few-fold, but only within a radius $r_{\rm res}$ enclosing a mass $\sim 0.1 M_\bullet$ of stars. The corresponding energy $\mathscr{E}_{\rm res}$ is marked on Fig. 2. Because $F^{\rm lc}(\mathscr{E}_{\rm res})$ is relatively small, the enhancement owing to resonant relaxation will not result in a significant increase in the total consumption rate.

Integrating over $\mathscr{E}$, the total consumption rate for the edge-on solar-composition model of M32 is $F^{\rm lc}_\odot = 7.6 \times 10^{-5}\,{\rm yr}^{-1}$. For the more realistic mass function described in Appendix A, this translates to a flaring rate $F^{\rm lc}_{\rm MF} = 1.3 \times 10^{-4}\,{\rm yr}^{-1}$. As noted in Section 2, the DF (and therefore the flaring rate) depends on the assumed inclination angle i of the galaxy. The probability ${\rm p}(i|q')$ that a galaxy of observed flattening q' has inclination i is given by equation (6) of Paper I. Using this to integrate the flaring rates for M32 over all i gives a mean rate $F^{\rm lc}_{\rm MF} = 1.2 \times 10^{-4}\,{\rm yr}^{-1}$. For M87, the 'consumption' rate $F^{\rm lc}_\odot = 2.1 \times 10^{-6}\,{\rm yr}^{-1}$, but, because only giant stars are disrupted outside the horizon of its BH, the more interesting visible 'flaring' rate is a mere $F^{\rm lc}_{\rm MF} = 7.9 \times 10^{-9}\,{\rm yr}^{-1}$.

Table 1 lists both $F^{\rm lc}_\odot$ and $F^{\rm lc}_{\rm MF}$ for all galaxies in Paper I with best-fitting $M_\bullet > 0$. Fig. 3 plots each as a function of bulge luminosity L. The rate is controlled by the density of stars at $\mathscr{E}_{\rm h}$, so that compact galaxies with steep 'power-law' central density cusps (Lauer et al. 1995) have the highest flaring rates, of up to about $10^{-4}\,{\rm yr}^{-1}$, while brighter, less dense 'core' galaxies like M87 have lower rates of about $10^{-8}\,{\rm yr}^{-1}$. Our values for $F^{\rm lc}_\odot$ are on average a factor of 4 larger than those calculated by Syer & Ulmer (1999) using less detailed models.

4 EFFECTS OF FLATTENING: THE LOSS WEDGE

4.1 Axisymmetry

The results of the previous section are based on the assumption that each galaxy is spherical, and therefore composed entirely of stars on centrophobic loop orbits. This is not the case, however, for more realistic non-spherical galaxies. Figs 4(a) and (b) show surfaces of section obtained by following orbits with $J_z = 0$, confined to the plane $y = 0$, in the potential of our axisymmetric edge-on model of M32, and plotting $Y \equiv J_y/J_{\rm c}$ versus colatitude θ at each apocentre passage. A significant portion of phase space in each case is occupied by centrophilic orbits, which cross the $Y = 0$ axis. The most tightly bound centrophilic orbits are regular 'lenses', which appear as bull's-eyes in Fig. 4(a) (Sridhar & Touma 1997). Further out (Fig. 4b) the centrophilic orbits become stochastic (Gerhard & Binney 1985).

The surfaces of section can be understood using the symplectic map of Touma & Tremaine (1997). Values (Y_n, θ_n) of (Y, θ) at successive apocentre passages are given by

$$\begin{aligned} Y_n' &= Y_n - \frac{1}{2}\epsilon \sin 2\theta_n \\ \theta_{n+1} &= \theta_n + g(Y_n') \\ Y_{n+1} &= Y_n' - \frac{1}{2}\epsilon \sin 2\theta_{n+1}. \end{aligned} \tag{25}$$

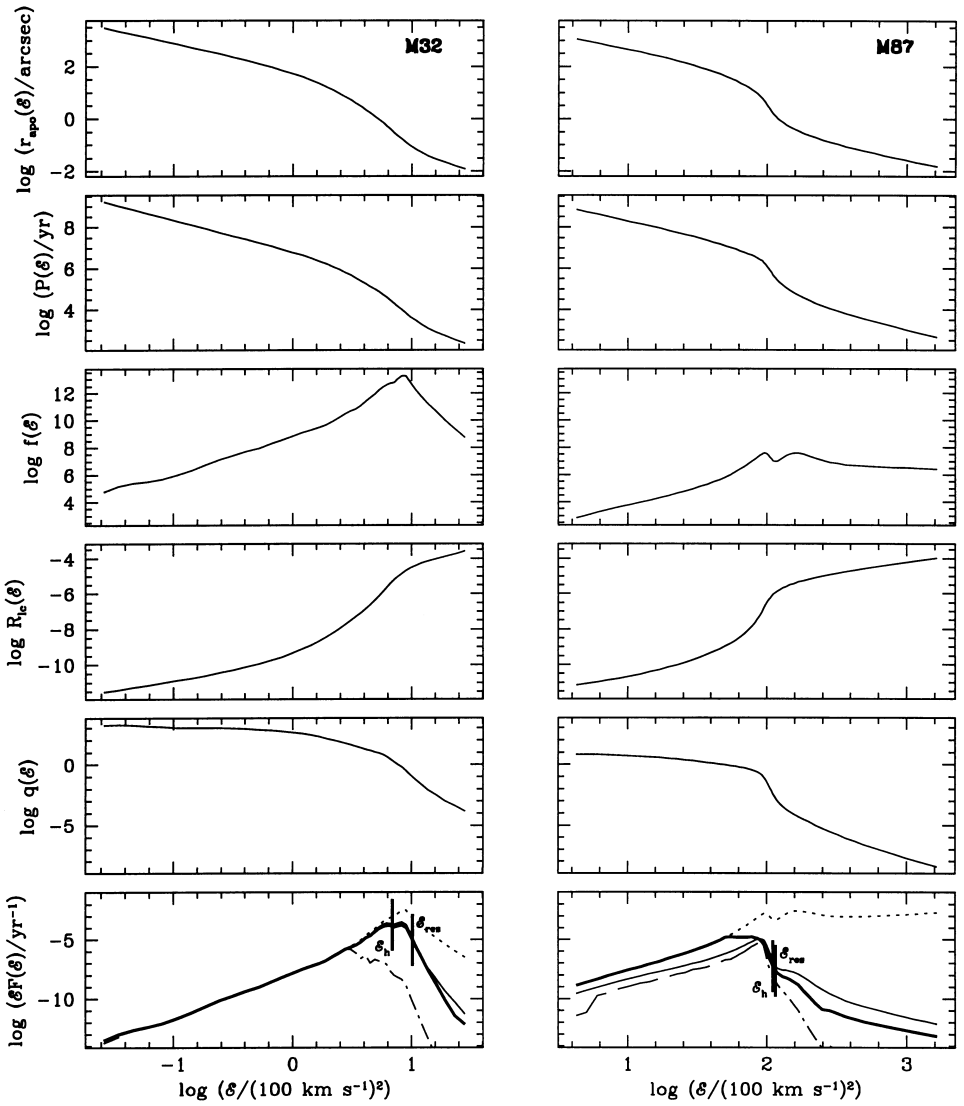

Figure 2. Diffusion of stars into the loss cones of M32 (left) and M87 (right), assuming that each is composed of stars of solar mass and radius. The top three panels on each side give the apocentre radius, orbital period $P(\mathscr{E})$ and DF $f(\mathscr{E})$ as functions of energy $\mathscr{E}$. Below these are the fraction $R_{\rm lc}(\mathscr{E}) \equiv J_{\rm lc}^2(\mathscr{E})/J_{\rm c}^2(\mathscr{E})$ of phase space occupied by the loss cone at a given energy, and the parameter $q(\mathscr{E})$ that distinguishes between the 'diffusion' ($q \ll -\ln R_{\rm lc}$) and 'pinhole' ($q \gg -\ln R_{\rm lc}$) régimes. The bottom panels plot the flux of stars into the BH's maw due to: a full loss cone, $F^{\rm full}(\mathscr{E})$ (Section 2 – dotted curves); two-body relaxation of stars into the loss cone, $F_\odot^{\rm lc}(\mathscr{E})$ (Section 3 – light full curves); draining of the loss wedge, $F_\odot^{\rm drain}(\mathscr{E}; 10^{10}\,{\rm yr})$ (Section 4 – dot-dashed curves); diffusion of stars into the loss wedge, $F_\odot^{\rm lw}(\mathscr{E})$ (Section 4 – dashed curves). The heavy full curve plots our final flux, $F_\odot(\mathscr{E})$, which is given by equation (51). $\mathscr{E}_{\rm res}$ marks the energy above which resonant relaxation becomes effective.

Here $\epsilon J_{\rm c}$ is the time-integral of the torque over one radial period, with

$$\epsilon = \frac{4}{J_{\rm c}} \int_{r_-}^{r_+} \frac{\psi_2(r)\,{\rm d}r}{[2(\psi(r) - \mathscr{E}) - Y^2 J_{\rm c}^2/r^2]^{1/2}}, \tag{26}$$

where ψ_2 is the $\cos 2\theta$ component of the potential, and

$$g(Y) = 2YJ_{\rm c} \int_{r_-}^{r_+} \frac{{\rm d}r}{r^2\{2[\psi(r) - \mathscr{E}] - Y^2 J_{\rm c}^2/r^2\}^{1/2}} \tag{27}$$

is the advance in θ per radial period. Touma & Tremaine demonstrate that this mapping provides a faithful representation of orbit structure in scale-free potentials. We find that it works just as well for our models of real galaxies.

These centrophilic orbits can have a dramatic effect on the consumption rate, because stars with $J \gg J_{\rm lc}$ can precess into the loss cone so long as $|J_z| < J_{\rm lc}$. Crudely speaking, the loss cone of the previous section is replaced by a loss 'wedge' with the same extent $|J_z| < J_{\rm lc}$ in the J_z direction of phase space, but stretched in the J direction to some $J_l \gg J_{\rm lc}$.

To investigate this process, we work with the canonical coordinate-momentum pairs (J_z, ϕ) and (J_θ, θ), where θ and ϕ are the usual angles in spherical coordinates and $J_\theta = r^2\dot{\theta}$. The total angular momentum is given by

$$J^2 = \frac{J_z^2}{\sin^2\theta} + J_\theta^2. \tag{28}$$

We are interested in the case $J_{\rm c} \gg |J_\theta| \gg J_{\rm lc} > |J_z|$, and we shall assume that the variations in J_θ are described by the Touma–Tremaine map (25) or approximations thereof. For $g(Y)$ $({\rm mod}\,\pi)$ small, the mapping is well approximated by motion under the averaged Hamiltonian

$$H = G(Y) - \frac{1}{2}\epsilon\cos 2\theta, \tag{29}$$

Table 1. Fuelling rates.

Galaxy	Type	D/Mpc	$\log\left(\frac{L_V}{L_\odot}\right)$	$\Upsilon_V/\Upsilon_\odot$	$\log\left(\frac{M_\bullet}{M_\odot}\right)$	r_h/arcsec	$\log(F^{lc}_\odot/yr^{-1})$	$\log(F^{lc}_{MF}/yr^{-1})$	$\log(F_\odot/yr^{-1})$	$\log(F_{MF}/yr^{-1})$	$\log(r_{apo}/arcsec)$
M31	S∩	0.8	9.860	4.8	7.792	4.19	-5.18 ± 0.11	-6.23 ± 0.12	-5.06 ± 0.08	-4.68 ± 0.07	1.90 ± 0.35
M32	E\	0.8	8.572	2.2	6.376	0.33	-4.15 ± 0.10	-3.91 ± 0.11	-3.91 ± 0.02	-3.62 ± 0.02	-0.40 ± 0.48
NGC 821	E\	19.5	10.188	8.3	8.298	0.17	-4.79 ± 0.13	-7.20 ± 0.13	-4.48 ± 0.08	-5.18 ± 0.09	0.49 ± 0.41
NGC 1399	E∩	17.9	10.616	7.8	9.718	2.57	-5.29 ± 0.20	-7.72 ± 0.20	-3.92 ± 0.34	-4.51 ± 0.34	1.09 ± 0.28
NGC 1600	E∩	50.2	11.012	12.1	10.059	1.61	-6.12 ± 0.09	-8.55 ± 0.09	-3.84 ± 0.04	-4.43 ± 0.04	0.75 ± 0.18
NGC 2300	E∩	31.8	10.660	8.8	9.454	1.13	-5.66 ± 0.09	-8.09 ± 0.09	-4.34 ± 0.06	-4.93 ± 0.06	0.71 ± 0.27
NGC 2832	E∩	90.2	11.112	7.6	10.058	0.97	-5.86 ± 0.09	-8.30 ± 0.09	-3.92 ± 0.10	-4.51 ± 0.10	0.48 ± 0.24
NGC 3115	S0\	8.4	10.232	8.0	8.608	0.35	-4.24 ± 0.08	-6.64 ± 0.08	-3.95 ± 0.05	-5.30 ± 0.05	0.80 ± 0.50
NGC 3377	E\	9.9	9.812	2.8	7.786	0.14	-4.19 ± 0.66	-4.98 ± 0.26	-3.94 ± 0.30	-4.48 ± 0.13	-0.41 ± 0.84
NGC 3379	E∩	9.9	10.152	5.3	8.594	0.56	-5.07 ± 0.13	-7.49 ± 0.13	-4.88 ± 0.06	-5.32 ± 0.07	1.06 ± 0.30
NGC 3608	E∩	20.3	10.268	5.9	8.392	0.23	-4.88 ± 0.02	-7.29 ± 0.02	-4.67 ± 0.15	-5.13 ± 0.07	0.63 ± 0.31
NGC 4168	E∩	36.4	10.636	5.9	9.077	0.68	-5.94 ± 0.17	-8.36 ± 0.18	-4.84 ± 0.05	-5.36 ± 0.04	0.59 ± 0.29
NGC 4278	E∩	17.5	10.396	5.7	9.166	1.24	-5.34 ± 0.05	-7.76 ± 0.05	-4.65 ± 0.07	-5.28 ± 0.08	0.91 ± 0.30
NGC 4291	E∩	28.6	10.272	6.3	9.271	0.81	-5.29 ± 0.03	-7.71 ± 0.03	-4.56 ± 0.02	-5.22 ± 0.03	0.65 ± 0.30
NGC 4472	E∩	15.3	10.960	9.0	9.417	1.08	-5.36 ± 0.20	-7.79 ± 0.20	-4.43 ± 0.13	-5.01 ± 0.14	1.16 ± 0.28
NGC 4473	E∩	15.8	10.252	5.1	8.533	0.21	-5.35 ± 0.14	-7.76 ± 0.15	-4.80 ± 0.02	-4.75 ± 0.15	0.52 ± 0.29
NGC 4486	E∩	15.3	10.884	10.8	9.558	1.70	-5.67 ± 0.15	-8.10 ± 0.15	-4.17 ± 0.22	-4.75 ± 0.22	1.42 ± 0.31
NGC 4486b	E∩	15.3	8.960	3.6	8.963	2.23	-5.64 ± 0.18	-8.06 ± 0.19	-5.32 ± 0.26	-6.23 ± 0.37	0.68 ± 0.40
NGC 4552	E∩	15.3	10.352	6.8	8.668	0.29	-4.88 ± 0.06	-7.30 ± 0.06	-4.91 ± 0.08	-5.57 ± 0.11	1.02 ± 0.34
NGC 4564	E\	15.3	9.908	5.3	8.404	0.03	-4.26 ± 0.44	-4.51 ± 1.53	-4.25 ± 0.31	-4.20 ± 1.21	-0.30 ± 0.76
NGC 4594	S0\	9.2	10.644	6.5	8.811	0.73	-5.26 ± 0.08	-7.68 ± 0.08	-4.67 ± 0.05	-5.31 ± 0.04	0.96 ± 0.38
NGC 4621	E\	15.3	10.440	7.0	8.445	0.14	-4.26 ± 0.14	-6.66 ± 0.14	-4.05 ± 0.06	-5.21 ± 0.15	0.67 ± 0.46
NGC 4636	E∩	15.3	10.600	8.1	8.356	0.28	-5.47 ± 0.10	-7.80 ± 0.08	-5.60 ± 0.07	-5.43 ± 0.14	1.04 ± 0.30
NGC 4649	E∩	15.3	10.788	8.6	9.592	1.75	-5.49 ± 0.01	-7.91 ± 0.01	-4.21 ± 0.18	-4.80 ± 0.19	1.19 ± 0.26
NGC 4660	E\	15.3	9.476	4.5	8.446	0.07	-3.81 ± 0.42	-5.05 ± 0.83	-3.85 ± 0.26	-4.63 ± 0.59	-0.13 ± 0.90
NGC 4874	E∩	93.3	11.348	9.2	10.319	2.24	-6.20 ± 0.11	-8.64 ± 0.11	-4.00 ± 0.09	-4.59 ± 0.09	0.76 ± 0.20
NGC 4889	E∩	93.3	11.276	6.4	10.429	2.49	-6.36 ± 0.10	-8.79 ± 0.10	-3.67 ± 0.07	-4.26 ± 0.07	0.61 ± 0.17
NGC 6166	E∩	112.5	11.320	7.7	10.467	3.95	-6.65 ± 0.04	-9.09 ± 0.04	-4.14 ± 0.04	-4.74 ± 0.04	0.76 ± 0.21
NGC 7768	E∩	103.1	11.104	6.9	9.933	0.87	-5.90 ± 0.07	-8.33 ± 0.06	-4.07 ± 0.08	-4.66 ± 0.08	0.33 ± 0.29

The second column gives the galaxy type: 'S0' = lenticular, 'S' = spiral bulge, 'E' = elliptical; '$\bigcap$' = cored, '\' = power law (Lauer et al. 1995). The distance D, luminosity L_V, best-fitting mass-to-light ratio Υ_V and black hole mass $M_\bullet$ for each galaxy are taken from Paper I (which assumes $H_0 = 80\,km\,s^{-1}\,Mpc^{-1}$). r_h is the radius of the sphere of influence of the BH. $F^{lc}_\odot$ is the steady-state rate stars drift into the loss cone by two-body relaxation (Section 3), neglecting the effects of centrophilic orbits and assuming that all stars have solar mass and radius. F^{lc}_{MF} is the more interesting visible flaring rate, calculated using the stellar mass function described in Appendix A. $F_\odot$ and F_{MF} are the rates obtained when the effects of both two-body relaxation and of centrophilic orbits (Section 4) are included. The errors give the uncertainties owing to the unknown inclination angle of each galaxy; the real uncertainties are much larger. The last column lists the mean and standard deviation of the distribution of the logarithm of the apocentre radii of the disrupted stars.

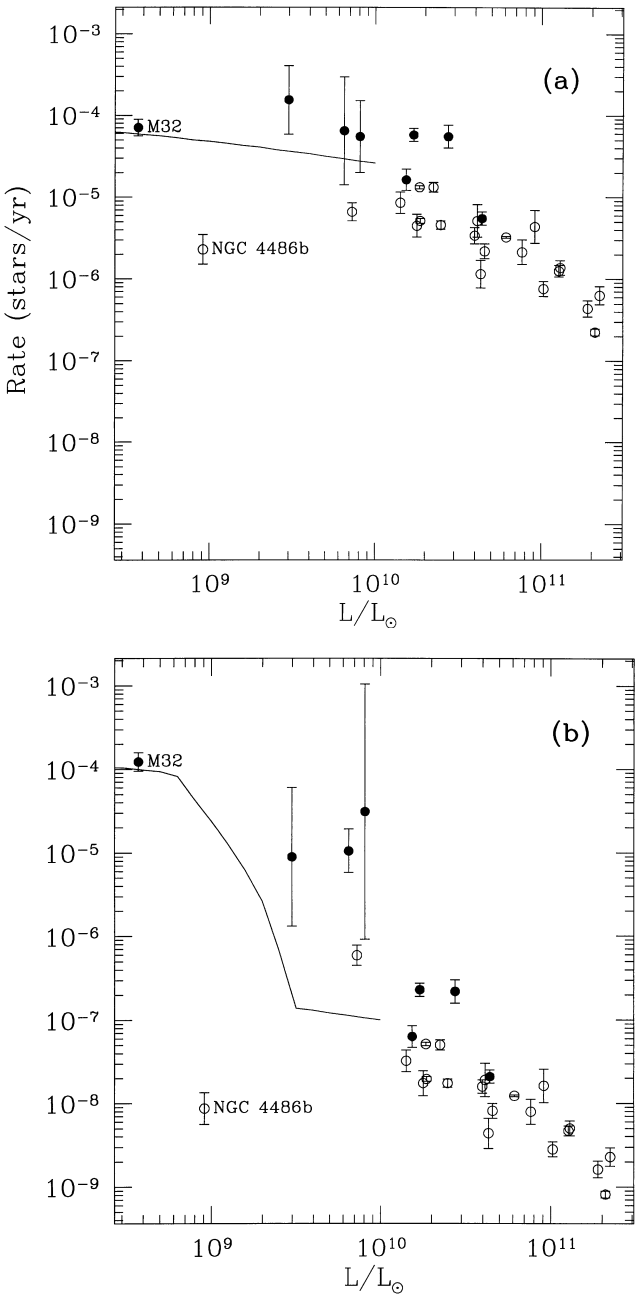

Figure 3. Consumption rates owing to two-body relaxation, plotted as a function of bulge luminosity. The panel on the left shows the consumption rate $F_{\odot}^{\rm lc}$ (equation 23) assuming that each galaxy is composed of stars of solar mass and radius. The one on the right shows the more interesting visible flaring rate $F_{\rm MF}^{\rm lc}$ assuming a more realistic mass function (Appendix A). Power-law and core galaxies (Lauer et al. 1995) are plotted as filled and open circles respectively. The error bars give the uncertainty in the rates due to the unknown inclination angle; the real uncertainties are much larger. The curves plot the rates predicted for the toy models described in Section 6.

where $Y = J_\theta/J_{\rm c}$, $|Y| \ll 1$ and

$$G(Y) \equiv \int_0^Y [g(Y') - g(0)]\,{\rm d}Y'. \tag{30}$$

For most realistic galaxy models (e.g. central black hole plus star density $\rho(r) \propto r^{-\gamma}$, with $\gamma < \frac{5}{2}$), $g(0) = 2\pi$ and $g'(0)$ is finite and negative. Thus we may write

$$G(Y) \simeq -\frac{1}{2}|g'(0)|Y^2, \tag{31}$$

and the motion in the (Y, θ) plane is approximately that of a simple pendulum:

$$Y^2(\theta) = Y_0^2 - Y_{\rm m}^2 \cos^2\theta. \tag{32}$$

Here Y_0 is the peak angular momentum of the orbit, and $Y_{\rm m}$ is the peak angular momentum of the $H = -\frac{1}{2}|\epsilon|$ separatrix orbit given by

$$|G(Y_{\rm m})| = |\epsilon|, \tag{33}$$

or, for small ϵ, $Y_{\rm m}^2 \simeq 2|\epsilon|/|g'(0)|$. Relativistic precession will cause the pericentre of an orbit with semimajor axis a and eccentricity e to advance by an additional amount $\Delta\theta \simeq 3\pi r_{\rm S}/a(1-e^2) \simeq \frac{3}{2}\pi Y_{\rm S}^2/Y^2$ per radial period, where $Y_{\rm S}J_{\rm c}$ is the angular momentum of an orbit with pericentre at the Schwarzshild radius $r_{\rm S}$. This has negligible effect on our calculation of $Y_{\rm m}$ using equation (33) because all our galaxies have $Y_{\rm m} \gg Y_{\rm S}$ (e.g. Fig. 4).

This averaged description of the motion does not work, however, below some critical energy $\mathscr{E}_{\rm s}$ where the centrophilic orbits become stochastic, as in Fig. 4(b). $\mathscr{E}_{\rm s}$ can be estimated by linearizing the map (25) about $Y = 0$ and making a trivial change of variables, so that it becomes a symmetric version of the Chirikov–Taylor map (see, e.g., Lichtenberg & Lieberman 1992 for extensive discussion). The condition for global stochasticity is (Touma & Tremaine 1997, equation 21)

$$|\epsilon| \gtrsim \frac{1}{2|g'(0)|}. \tag{34}$$

We calculate the area of the stochastic region of (J_θ,θ) phase space by iterating the map (25) starting from $Y = 0$ and a range of randomly chosen $\theta \in [0, \pi]$. The area of phase space occupied by stochastic orbits is then taken to be $2\pi J_l$, where J_l is twice the average value of $|J_\theta|$. We assume that orbits inside this stochastic region fill it uniformly. Although this approach is quite crude (for example, the estimate of the area can be affected by the presence of resonant 'boxlet' orbits described by Miralda-Escudé & Schwarzschild 1989), it is more than adequate for our purposes below.

4.1.1 *Draining a full loss wedge*

We first estimate the time required to drain the loss wedge, neglecting refilling by two-body relaxation or other processes. In the spirit of our two-integral assumption, let us suppose that at time $T = 0$ the number of stars in a small interval of phase space is $4\pi^2 P(\mathscr{E}) f(\mathscr{E})\,{\rm d}\mathscr{E}\,{\rm d}J_z\,{\rm d}J$ (cf. equation 6), and that the probability a given star is consumed in one radial period is p. Then after time T the loss wedge drains at a rate

$$F^{\rm drain}(\mathscr{E};T)\,{\rm d}\mathscr{E} = 4\pi^2 f(\mathscr{E})\,{\rm d}\mathscr{E}\int {\rm d}J_z\,{\rm d}J p(1-p)^{T/P(\mathscr{E})}. \tag{35}$$

After many orbits ($T \gg P(\mathscr{E})$, $p \ll 1$) this simplifies to

$$F^{\rm drain}(\mathscr{E};T)\,{\rm d}\mathscr{E} = 4\pi^2 f(\mathscr{E})\,{\rm d}\mathscr{E}\int {\rm d}J_z\,{\rm d}J p\exp[-pT/P(\mathscr{E})]. \tag{36}$$

We must now estimate the consumption probability p, equal to the fractional time that the star spends with total angular momentum $J < J_{\rm lc}$. We first consider the case of a star on a

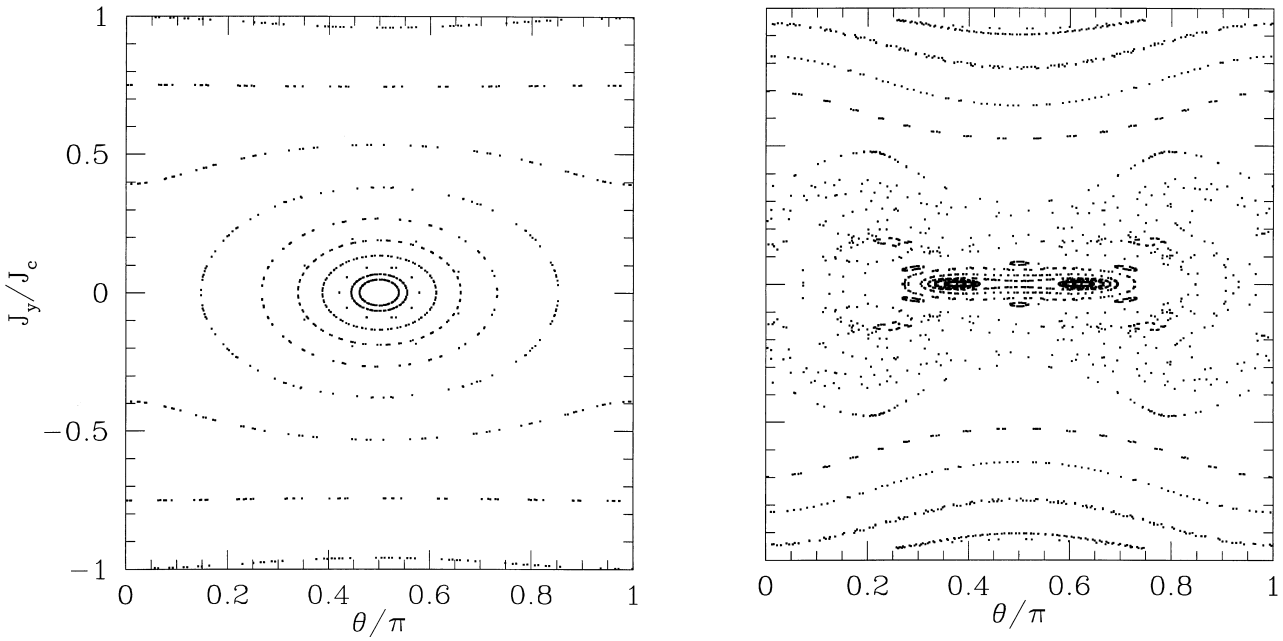

Figure 4. Surfaces of section of $J_z = 0$ orbits in our edge-on model of M32 obtained by plotting J_y/J_c versus colatitute θ at each apocentre passage. The panel on the left (right) plots orbits with energies equal to that of a radial orbit with apocentre radius 1 pc (3 pc). The bull's-eyes on the left are lens orbits (Sridhar & Touma 1997).

regular orbit (equation 32). Although these trajectories can be written explicitly in terms of elliptic integrals, for the sake of simplicity we shall work with approximate orbits valid for $Y_0 \ll Y_m$:

$$J_\theta = J_0 \sin\psi, \qquad \theta = \frac{1}{2}\pi + \frac{J_0}{J_m}\cos\psi, \tag{37}$$

where $J_0 = J_c Y_0$, $J_m = J_c Y_m$, and ψ is a phase angle that increases linearly with time. Therefore,

$$p \simeq \frac{2}{\pi}\sin^{-1}\left(\frac{\sqrt{J_{lc}^2 - J_z^2}}{J_0}\right) \simeq \frac{2\sqrt{J_{lc}^2 - J_z^2}}{\pi J_0}, \tag{38}$$

for $J_{lc} \ll J_0 < J_m$ and $|J_z| < J_{lc}$, and zero otherwise.

Next we estimate the area of (J_θ, θ) phase space occupied by orbits with peak angular momenta lying between J_0 and $J_0 + \mathrm{d}J_0$. From equation (32), the area associated with lens orbits with peak angular momenta less than J_0 is $A(J_0)$, where $A(J_0) \simeq \pi J_0^2/J_m$ for $J_0 \ll J_m$ and $A(J_m) = 4J_m$. So, in equation (36) we may replace the area element $2\pi \mathrm{d}J$ by $\mathrm{d}A \simeq 2\pi J_0\,\mathrm{d}J_0/J_m$ (for $J_0 \ll J_m$).

With these results, equation (36) becomes

$$\begin{aligned} F^{\rm drain}(\mathscr{E};T)\,\mathrm{d}\mathscr{E} &= \frac{4\pi^2}{J_m} f(\mathscr{E})\,\mathrm{d}\mathscr{E}\int \mathrm{d}J_z J_0\,\mathrm{d}J_0 p\exp[-pT/P(\mathscr{E})] \\ &= 8\pi f(\mathscr{E})\,\mathrm{d}\mathscr{E}\int_{-J_{lc}}^{J_{lc}} \mathrm{d}J_z\sqrt{J_{lc}^2 - J_z^2} \\ &\quad \times \int_1^\infty \frac{\mathrm{d}x}{x^2}\exp\left[-\frac{2\sqrt{J_{lc}^2 - J_z^2}}{\pi J_m}\frac{Tx}{P(\mathscr{E})}\right], \end{aligned} \tag{39}$$

where $x = J_m/J_0$. For times $T \ll P(\mathscr{E})J_m/J_{lc}$, the exponential is roughly unity, and we have

$$F^{\rm drain}(\mathscr{E};T)\,\mathrm{d}\mathscr{E} = 4\pi^2 J_{lc}^2 f(\mathscr{E})\,\mathrm{d}\mathscr{E}, \tag{40}$$

equal to the draining rate for a spherical system with full loss cone, $F^{\rm full}(\mathscr{E})$ (equation 12). For $T \gg P(\mathscr{E})J_m/J_{lc}$, the draining rate is dominated by stars with $J_{lc}^2 - J_z^2 \ll J_{lc}^2$, which give

$$F^{\rm drain}(\mathscr{E};T)\,\mathrm{d}\mathscr{E} = \frac{\pi^4 J_m^3}{J_{lc}}\left[\frac{P(\mathscr{E})}{T}\right]^3 f(\mathscr{E})\,\mathrm{d}\mathscr{E}; \tag{41}$$

the consumption rate declines as T^{-3} (in the absence of refilling of the loss wedge by two-body relaxation or other effects).

For stochastic ($\mathscr{E} < \mathscr{E}_s$) orbits we assume the orbits are uniformly distributed in the (J_θ, θ) plane for $|J_z| < J_l$. We then have from equation (28) that

$$p = \frac{1}{\pi J_l}\int \mathrm{d}\theta\left(J_{lc}^2 - \frac{J_z^2}{\sin^2\theta}\right)^{1/2}, \tag{42}$$

where the integral is taken over all $\theta \in [0, \pi]$ for which the radicand is positive, and $p = 0$ for centrophobic orbits with $|J_\theta| > J_l$. Then equation (36) yields

$$F^{\rm drain}(\mathscr{E};T)\,\mathrm{d}\mathscr{E} = 4\pi^2 f(\mathscr{E})\,\mathrm{d}\mathscr{E} J_l\int_{-J_{lc}}^{J_{lc}} \mathrm{d}J_z p\exp[-pT/P(\mathscr{E})]. \tag{43}$$

For times $T \ll P(\mathscr{E})J_l/J_{lc}$, the exponential is roughly unity. Substituting equation (42) and changing the order of integration, we recover equation (40). For $T \gg P(\mathscr{E})J_l/J_{lc}$, the draining rate is dominated by stars with $J_{lc} - |J_z| \ll J_{lc}$. In this case $p = (J_{lc} - |J_z|)/J_l$ and we find

$$F^{\rm drain}(\mathscr{E};T)\,\mathrm{d}\mathscr{E} = 8\pi^2 J_l^2\left[\frac{P(\mathscr{E})}{T}\right]^2 f(\mathscr{E})\,\mathrm{d}\mathscr{E}; \tag{44}$$

the consumption rate declines as T^{-2} and, remarkably, is independent of J_{lc}; only the time required to reach this asymptotic régime depends on J_{lc}.

4.1.2 *Refilling the loss wedge by two-body relaxation*

These results neglect refilling of the loss wedge by two-body

relaxation. The steady-state refilling rate can be calculated using a Fokker–Planck analysis similar to that of the previous section, but considering diffusion in J_z rather than in $R \equiv J^2/J_c^2$. To zeroth order in J_z, the frictional diffusion coefficient $\langle \Delta J_z \rangle = r \sin\theta \langle \Delta v_\phi \rangle = 0$, while the diffusion coefficient

$$D_z \equiv \frac{1}{2}\langle (\Delta J_z)^2 \rangle = \frac{1}{2} r^2 \sin^2\theta \langle (\Delta v_\phi)^2 \rangle \simeq \frac{1}{4}\mu J_c^2 \sin^2\theta, \tag{45}$$

where μ is the diffusion coefficient of the previous section. We shall average D_z over θ because in most galaxies the precession time is short compared with the relaxation time; thus $\bar{D}_z = \frac{1}{8}\mu J_c^2$.

For regular $\mathscr{E} > \mathscr{E}_s$ orbits the (orbit-averaged) flux of stars through a surface of constant J_z is

$$\begin{aligned}\frac{1}{2}F^{\rm lw}(\mathscr{E})\,{\rm d}\mathscr{E} &= 2\pi \bar{D}_z P \int {\rm d}J_\theta\,{\rm d}\theta \frac{\partial f}{\partial J_z}{\rm d}\mathscr{E} \\ &= 2\pi q_z J_{\rm lc}^2 A(J_{\rm m}) \frac{\partial f}{\partial J_z}{\rm d}\mathscr{E},\end{aligned} \tag{46}$$

where $q_z \equiv P\bar{D}_z/J_{\rm lc}^2$ and we have assumed that $\partial f/\partial J_z$ is approximately constant over the loss wedge. In terms of $q \equiv P\bar{\mu}/R_{\rm lc}$ used in the previous section, $q_z = q/8$. We include the factor of 1/2 on the left-hand side of equation (46) because orbits with $J_z = \pm J_{\rm lc}$ contribute identical amounts to the total flux into the loss wedge.

We assume that the galaxy is in a steady state, at least for small $|J_z| \ll J_c$. Then $F^{\rm lw}(\mathscr{E}, J_z)$ must be independent of J_z for $J_{\rm lc} < |J_z| \ll J_c$. Thus $f(\mathscr{E}, J_z) = a(\mathscr{E}) + b(\mathscr{E})|J_z|$. The rate of consumption of stars is given by equation (40) with $f(\mathscr{E}) = a(\mathscr{E})$, and this must equal $F^{\rm lw}(\mathscr{E})$; therefore $a(\mathscr{E}) = q_z A(J_{\rm m}) b(\mathscr{E})/\pi$. The corresponding 'isotropized' DF is

$$\bar{f}(\mathscr{E}) \equiv \frac{b(\mathscr{E})}{J_c}\int_0^{J_c}\left(\frac{q_z A(J_{\rm m})}{\pi} + J_z\right){\rm d}J_z, \tag{47}$$

which is what one measures by inverting equation (7). Therefore, for $J_z \ll J_c$,

$$f(\mathscr{E}, J_z) = \bar{f}(\mathscr{E})\frac{1 + \pi|J_z|/(4q_z J_{\rm m})}{1 + \pi J_c/(8q_z J_{\rm m})}. \tag{48}$$

Substituting into equation (46), the steady-state consumption rate is

$$F^{\rm lw}(\mathscr{E})\,{\rm d}\mathscr{E} = 4\pi^2 J_{\rm lc}^2(\mathscr{E})\frac{\bar{f}(\mathscr{E})\,{\rm d}\mathscr{E}}{1 + \pi J_c/(8q_z J_{\rm m})}. \tag{49}$$

The boundary between the 'diffusion' and 'pinhole' régimes for the loss wedge occurs at $q_z \simeq 0.5 J_c/J_{\rm m}$ (i.e. $q \simeq 4J_c/J_{\rm m}$), rather than at $q \simeq -\ln R_{\rm lc}$ as in the case when the galaxy is composed purely of centrophobic loop orbits. In the pinhole limit $q_z \gg J_c/J_{\rm m}$, the consumption rate $F^{\rm lw}(\mathscr{E})$ is identical to $F^{\rm full}(\mathscr{E})$: the increase in the surface area of the loss wedge by a factor $\sim 4J_{\rm m}/J_{\rm lc}$ over that of the loss cone is exactly cancelled by the decrease in the consumption probability per star per radial period.

For stochastic ($\mathscr{E} < \mathscr{E}_s$) orbits, a similar calculation gives

$$F^{\rm lw}(\mathscr{E})\,{\rm d}\mathscr{E} = 4\pi^2 J_{\rm lc}^2(\mathscr{E})\frac{\bar{f}(\mathscr{E})\,{\rm d}\mathscr{E}}{1 + J_c/(4q_z J_l)}, \tag{50}$$

so that the boundary between diffusion and pinhole régimes occurs at $q_z \simeq 0.25 J_c/J_l$ (i.e. $q \simeq 2J_c/J_l$). Equations (49) and (50) are identical when expressed in terms of the area of (J_θ, θ) phase space occupied by centrophilic orbits [$2\pi J_l$ and $A(J_{\rm m}) = 4J_{\rm m}$, respectively].

The dashed curves in Fig. 2 show $F_\odot^{\rm lw}(\mathscr{E})$ for our edge-on models of M32 and M87. The small differences between $F_\odot^{\rm lw}(\mathscr{E})$ and the corresponding $F_\odot^{\rm lc}(\mathscr{E})$ are due solely to the differences between the steady-state solutions for the two-dimensional loss-cone problem [in which $f(J) \propto \ln(J^2/J_0^2)$] and the one-dimensional loss-wedge problem [where $f(J_z) \propto a + b|J_z|$]. Taking all the galaxies in our sample, we find that on average $F_\odot^{\rm lw}$ is greater than $F_\odot^{\rm lc}$ by a factor of 1.8, although this ratio can be as large as 5 for the most face-on, flattened models in which a large portion of (J_θ, θ) phase space is occupied by centrophilic orbits. The actual value of $F^{\rm lw}$ itself typically only increases by about 40 per cent from the edge-on model of a given galaxy to the most face-on, flattened model, because the flatter model has fewer stars on low-angular momentum orbits.

The dot–dashed curves in Fig. 2 show $F_\odot^{\rm drain}(\mathscr{E})$ assuming that both galaxies have an 'age' $T = 10^{10}$ yr. In moderately large ($L \gtrsim 10^{10}\,{\rm L}_\odot$) galaxies, a significant fraction of giant stars on centrophilic orbits may linger in the loss wedge for longer than 10^{10} yr. This fossil population can increase the flaring rates in these large galaxies by orders of magnitude over $F_{\rm MF}^{\rm lw}$.

Our final fuelling rate is

$$F(\mathscr{E}) = \max[F^{\rm lw}(\mathscr{E}), F^{\rm drain}(\mathscr{E}; 10^{10}\ {\rm yr})]. \tag{51}$$

For each of the galaxies in Paper I with $M_\bullet > 0$, Table 1 lists both the 'consumption' rate $F_\odot$ assuming the galaxy is composed of stars of solar mass and radius, and the visible flaring rate $F_{\rm MF}$ assuming the more sensible stellar mass function of Appendix A. Fig. 5 plots these rates as a function of bulge luminosity. Table 1 also lists the mean and standard deviation of the distribution of the logarithm of the apocentre radii of the disrupted stars; we see that most of the consumption is from radii $\gtrsim 1$ arcsec, where the spatial distribution of stars is well-determined by the observations.

4.2 Triaxiality

Similar arguments can be applied to triaxial galaxies. Once again, there will be some characteristic minimum angular momentum $J_s(\mathscr{E})$ inside which most orbits are no longer loops, but centrophilic. We suppose that at time $T = 0$ the number of stars on centrophilic orbits is $N(\mathscr{E})J_s^2/J_c^2 \simeq 4\pi^2 P J_s^2 f(\mathscr{E})$. Most of these orbits will be stochastic. The probability that a given star on such an orbit will be tidally consumed within a radial orbital period is $J_{\rm lc}^2/J_s^2$. Then, after time T the consumption rate is

$$F^{\rm triax}(\mathscr{E})\,{\rm d}\mathscr{E} = 4\pi^2 f(\mathscr{E}) J_{\rm lc}^2(\mathscr{E}) \exp\left[-\frac{T}{P(\mathscr{E})}\frac{J_{\rm lc}^2(\mathscr{E})}{J_s^2(\mathscr{E})}\right]{\rm d}\mathscr{E}. \tag{52}$$

The refilling of the loss region can be described using equations similar to those in Section 4.1.2.

These arguments assume that the potential of the galaxy remains fixed. In reality, the galaxy becomes slowly more axisymmetric from the centre out, owing to the action of the stochastic orbits. Merritt & Quinlan (1998) find that, for all but the most puny BHs, at any given radius the galaxy becomes axisymmetric within $\sim 10^2$ local orbital periods. So, after time T we may take $J_s(\mathscr{E}) = 0$ for $\mathscr{E} > \mathscr{E}_s$, where $10^2 P(\mathscr{E}_s) = T$. For all our galaxies we find that $F^{\rm triax}(\mathscr{E}) < F(\mathscr{E})$, so that the additional effects of triaxiality are negligible compared with those of axisymmetry.

5 CONTRIBUTION OF CONSUMED STARS TO $M_\bullet$

The mass of stars in a full loss wedge ranges from about $10^4\,{\rm M}_\odot$

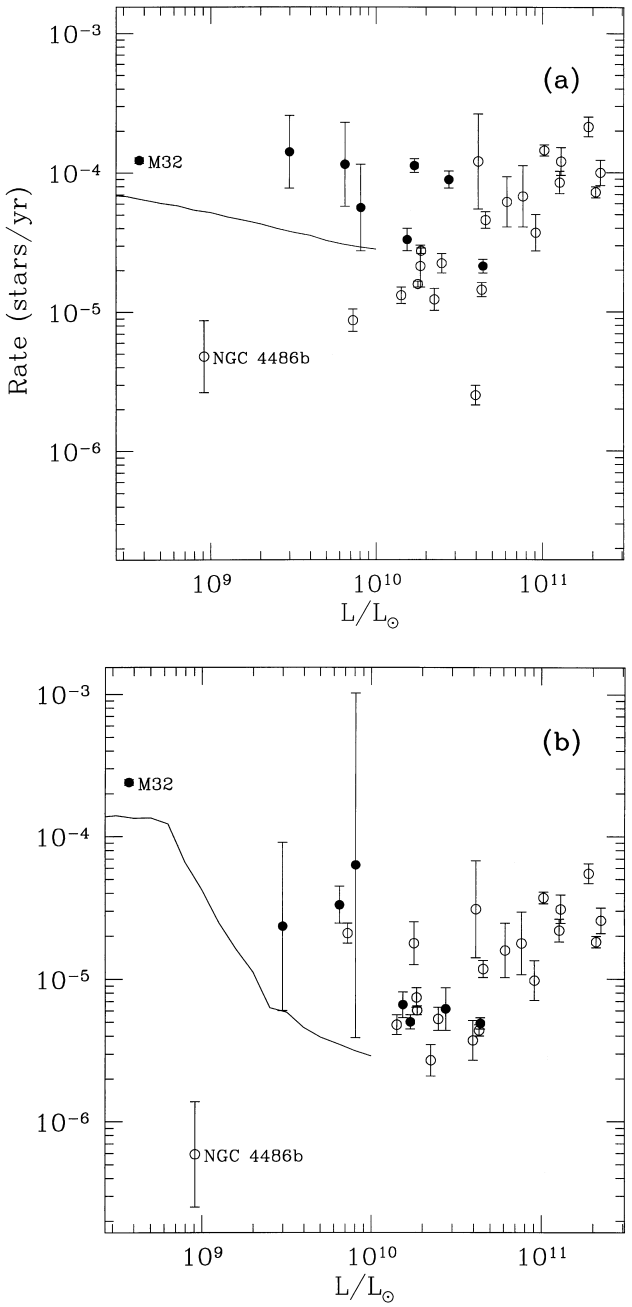

Figure 5. As for Fig. 3, but plotting total consumption rates (equation 51) taking account of flattening and two-body relaxation. The panel on the left shows the consumption rate $F_\odot$ assuming that each galaxy is composed of stars of solar mass and radius. The one on the right shows the visible flaring rate $F_{\rm MF}$ assuming the more realistic mass function in Appendix A. Power-law and core galaxies (Lauer et al. 1995) are plotted as filled and open circles respectively. The error bars give the uncertainty in the rates due to the unknown inclination angle; the real uncertainties are larger. The curves plot the rates for the toy models described in Section 6.

for small compact galaxies (with $M_\bullet \sim 10^6\,{\rm M}_\odot$) up to about $10^7\,{\rm M}_\odot$ for the largest galaxies (with $M_\bullet \sim 10^{10}{\rm M}_\odot$). Thus we can neglect the contribution of $F^{\rm drain}$ to the growth of a central BH, and estimate the contribution of consumed stars to $M_\bullet$ by

$$M^{\rm eaten} \sim F^{\rm lw}_\odot T\,{\rm M}_\odot, \tag{53}$$

where T is the age of the galaxy. Taking $T = 10^{10}$ yr, Fig. 5(a) shows that $M^{\rm eaten} \sim 10^6\,{\rm M}_\odot$, independent of galaxy luminosity. Only for the most compact galaxies (e.g. only for M32 in our sample) has the consumption of stars had any significant effect on the mass of the BH. This result also implies that in most galaxies the capture of stars is not strong enough to spin down the BH (e.g. Young 1977; Beloborodov et al. 1992).

6 DETECTING FLARES IN SURVEYS

The sample of Paper I is strongly biased towards rare bright galaxies, but nevertheless we can still use it to estimate the flaring rate per unit volume. Ferguson & Sandage (1991) find that the luminosity function of E + S0 galaxies in each of four nearby clusters is well described by the Gaussian

$$N(L)\,{\rm d}\log L = \frac{N_0}{\sqrt{2\pi}\Delta}\exp\left[-\frac{1}{2}\left(\frac{\log L - \log L_0}{\Delta}\right)^2\right]{\rm d}\log L, \tag{54}$$

where $\Delta = 0.6$, $L_0 = 1.3\times10^9\,h^{-2}\,{\rm L}_\odot$ in the B band and h is the Hubble constant in units of $100\,{\rm km\,s^{-1}\,Mpc^{-1}}$. (The corresponding mean V-band luminosity $L_0 = 1.9\times10^9 h^{-2}\,{\rm L}_\odot$, assuming that $B - V = 1$.) We assume that this luminosity function also provides a good description of field galaxies (Sandage, Tammann & Yahil 1979). We estimate N_0 using the B-band luminosity function found by Efstathiou, Ellis & Peterson (1988), noting that, from their table 4, approximately one third of all galaxies brighter than about $10^9 h^{-2}\,{\rm L}_\odot$ are of type E or S0. This yields $N_0 = 8.3\times10^{-3}\,h^3\,{\rm Mpc^{-3}}$. The corresponding mean B-band luminosity density of field E + S0 galaxies is then $2.8\times10^7\,h\,{\rm L}_\odot\,{\rm Mpc^{-3}}$. For comparison, the luminosity density of dE + E + S0 galaxies is $4.4\times10^7\,h\,{\rm L}_\odot\,{\rm Mpc^{-3}}$ (Yahil, Sandage & Tammann 1980) and the luminosity density of all hot components (E + S0 galaxies and spiral bulges) is $5.4\times10^7\,h\,{\rm L}_\odot\,{\rm Mpc^{-3}}$, estimated using Efstathiou et al.'s (1988) mean galaxy luminosity density $j = 1.8\times10^8\,h\,{\rm L}\odot\,{\rm Mpc^{-3}}$ and Schechter & Dressler's (1987) result that bulges contribute approximately 30 per cent to this (see also appendix B of Faber et al. 1997).

Figs 3 and 5 hint that the consumption rates are roughly constant functions of L. We now show that this is indeed the case by using known correlations of galaxy properties to construct a sequence of toy galaxy models and calculating their consumption rates. Following Paper I, we assume that every bulge has a BH of mass

$$M_\bullet = 6.1\times10^8\,h^{-1}\left(\frac{L}{10^{10}\,h^{-2}\,{\rm L}\odot}\right)^{1.17}{\rm M}_\odot, \tag{55}$$

and a stellar mass-to-light ratio

$$\Upsilon_V = 6.6\,h\left(\frac{L}{10^{10}\,h^{-2}\,{\rm L}_\odot}\right)^{0.18}\Upsilon_\odot. \tag{56}$$

Galaxies with $L \lesssim 2\times10^9\,h^{-2}\,{\rm L}_\odot$ ($M_\bullet \lesssim 10^8\,{\rm M}_\odot$) will dominate the consumption rate (Fig. 5). These galaxies have steep power-law central density cusps (Faber et al. 1997), which we approximate using an E2 Jaffe (1983) model. For the effective radius of each model we take

$$R_{\rm eff} = 2.4\,h^{-1}\left(\frac{L}{10^{10}\,h^{-2}\,{\rm L}_\odot}\right)^{0.65}{\rm kpc}, \tag{57}$$

obtained by fitting to the galaxies in Faber et al. (1997). We find

that

$$F_{\odot}(L) = 2.7\times10^{-5}\,h^{2/3}\left(\frac{L}{10^{10}\,h^{-2}\,\mathrm{L}_{\odot}}\right)^{-0.22}\ \mathrm{yr}^{-1}, \qquad (58)$$

almost independent of luminosity. We plot this consumption rate $F_{\odot}(L)$ and the flaring rate $F_{\rm MF}(L)$ for these toy models on Fig. 5 [and also $F^{\rm lc}_{\odot}(L)$ and $F^{\rm lc}_{\rm MF}(L)$ on Fig. 3]. They are broadly consistent with the rates calculated for real galaxies, given the small number of the latter with $L \lesssim 10^{10}\,\mathrm{L}_{\odot}$, and our neglect of the substantial scatter in the relation between $M_{\bullet}$ and L. Integrating $F_{\rm MF}(L)$ of the toy model weighted by the luminosity function (54) gives a flaring rate per unit volume of $7.5\times10^{-7}h^{11/3}\,\mathrm{yr}^{-1}\,\mathrm{Mpc}^{-3}$ for E + S0 galaxies.

There is currently little evidence for or against the presence of BHs in the centres of late-type bulge-less spiral galaxies, but BHs do appear to be common features in bulges of type Sbc and earlier (Richstone et al. 1998). These early-type spirals have approximately the same luminosity distribution (54) as E + S0 galaxies, and are about as common (Binggeli, Sandage & Tammann 1988; see also above). Neither of the two spirals (M31 and NGC 4594) in Paper I show any peculiarities in their consumption rates compared with the other E + S0 galaxies. Therefore, we multiply the flaring rate for E + S0 galaxies by 2 to obtain a total flaring rate per unit volume of $1.5\times10^{-6}h^{11/3}\,\mathrm{yr}^{-1}\,\mathrm{Mpc}^{-3}$.

There are a couple of major uncertainties in this rate, over and above those we discuss in the next section. First, the evidence for our assumed $M_{\bullet}$–L correlation (55) is slight for $L \lesssim 10^{10}\,\mathrm{L}_{\odot}$. Secondly, the density profiles of real galaxies may not follow the steep $\nu\sim r^{-2}$ profile of our assumed Jaffe models close to their centres. For example, the density profile of M32 is observed to turn over at small radii (Section 2). Modelling it with a Jaffe profile would overestimate $F^{\rm lw}$ by about a factor of 2.

According to the thick disc models of Ulmer (1999), disruption of a solar-type star by a $10^6\,\mathrm{M}_{\odot}$ ($10^7\,\mathrm{M}_{\odot}$) BH should create a flare with V-band luminosity of at least $2\times10^7\,\mathrm{L}_{\odot}$ ($8\times10^8\,\mathrm{L}_{\odot}$). From the correlation (58), these BH masses correspond to host bulge V-band luminosities of $3\times10^8\,\mathrm{L}_{\odot}$ ($1.3\times10^9\,\mathrm{L}_{\odot}$) – thus the flare luminosity is about 10 to 60 per cent of the luminosity of the surrounding bulge. In the U-band the flares outshine the galaxy by at least a factor of 4. Thus, rather than monitoring the nearest 10^5 or so closest candidate galaxies for evidence of flares, it would be much more economical to survey small areas of the sky deeply, as is done in current supernovae searches (e.g. Pain et al. 1996). For a survey sensitive to all flares within a redshift z, the expected detection rate is approximately

$$0.11\,h^{2/3}\left(\frac{z}{0.3}\right)^3 \ \text{per square deg per yr}, \qquad (59)$$

with an uncertainty of at least a factor of 2. This flaring rate is about 0.01 times the Type Ia supernova rate.

In their R-band survey, Pain et al. (1996) can just detect a supernova of apparent magnitude 21.8 in the centre of a galaxy of magnitude 20.8 (their fig. 1). Thus the brightest flares, yielding a 40 per cent increase in the luminosity of a $L_V = 2\times10^9\,\mathrm{L}_{\odot}$ galaxy, are just detectable out to $z = 0.3$, and an R-band survey will not yield more than about one flare per $10\,\mathrm{deg}^2$ per yr. It might be possible to carry out significantly deeper searches in the V band (corresponding to the rest-frame U band of the flares).

These results imply that a flare with $L\sim10^{7.5}\,\mathrm{L}_{\odot}$ occurred in the centre of M32 within the last 10^4 yr or so. At present there is no evidence for non-thermal emission from the centre of M32: *HST* photometry shows no significant evidence for a colour gradient in the central pixel (Lauer et al. 1998), setting an upper limit of $\sim10^{4.5}\,\mathrm{L}_{\odot}$ to any non-thermal source. Thus the flare luminosity must decay by at least a factor of 10^3 over 10^4 yr.

7 POSSIBLE SHORTCOMINGS OF THE MODELS

The models above are based on some quite strong assumptions. Here we discuss a number of ways in which real galaxies might differ from the models.

Anisotropy: Our two-integral assumption is most reasonable for power-law galaxies, because their rapid rotation limits the amount of radial anisotropy they may have. No such constraint exists for larger core galaxies which tend to rotate slowly, if at all. Any increase in the number of stars on very low-J orbits will obviously enhance the flaring rates. Recent models (Merritt & Oh 1997; Rix et al. 1997; Gerhard et al. 1998) suggest that core galaxies could have σ_r^2/σ_ϕ^2 lying between 1.2 and 1.4 (under the assumption of spherical symmetry). However, even detailed kinematic modelling of individual galaxies can only yield information on their DFs for $J \gtrsim 0.1J_{\rm c} \gg J_{\rm lc}$, and thus does not greatly improve the reliability of estimates of flaring rates.

Tidal capture: The calculations of Sections 3 and 4 give rates for the *direct* disruption of stars. They neglect the possibility that stars that come within a few times $r_{\rm t}$ of the BH may be tidally captured by the BH and then disrupted during a subsequent pericentre passage (e.g. Frank & Rees 1976; Novikov, Pethick & Polnarev 1992; Diener et al. 1995). The radius for tidal capture is at most $\sim3r_{\rm t}$ (Novikov et al. 1992), and thus tidal capture could enhance the disruption rates by up to a factor of 3. Similar arguments apply to any dense extended disc (e.g. Norman & Silk 1983) that may surround the BH.

BH wandering: A BH can wander from the centre of the galaxy as a result of Poisson noise from the stellar distribution (Bahcall & Wolf 1976), weakly damped $l = 1$ lop-sided modes of oscillation (Weinberg 1994), an eccentric stellar disc (Tremaine 1995), or other processes; all of these are poorly understood. It is unclear what effect wandering would have on the fuelling rate. If the wandering time-scale is long compared to the orbital time-scales of stars, then clearly the resulting refilling of the loss wedge would result in an increase in the disruption rates. On the other hand, if the wandering time-scale is much shorter than the orbital time-scale and the BH has a typical displacement $r_0 \ll r_{\rm h}$ from the centre of the stellar distribution, then stars with pericentres within r_0 (rather than $r_{\rm t}$) can potentially be consumed. From equation (2), this is a factor $\sim r_0/r_{\rm t}$ more stars than if the BH stayed at the centre of the galaxy. But the probability that any given one of these stars will be consumed is only $\sim r_{\rm t}^2/r_0^2$, so that there would be a net *decrease* of $\sim r_{\rm t}/r_0$ in the consumption rate if the BH wandering were fast enough.

Other relativistic effects: Our calculations use $\eta = 0.844$ in equation (1) for $r_{\rm t}$. This value is based on Diener et al.'s (1995) Newtonian calculations, which strictly apply only for $M_{\bullet} \ll 10^8\,\mathrm{M}_{\odot}$. We have also assumed that stars for which $r_{\rm t} \gtrsim r_{\rm S}$ are consumed whole by the BH, without a visible flare. This only applies to Schwarzschild BHs. For Kerr BHs, Beloborodov et al. (1992) show that $r_{\rm t}$ depends on the direction at which the star approaches the BH, with the angle-averaged $r_{\rm t}$ approximately equal to the $r_{\rm t}$ obtained assuming a Schwarzschild BH. Thus a

spinning BH of mass $M_\bullet > 10^8\,\mathrm{M}_\odot$ could disrupt a main-sequence star that approaches from a favourable direction.

8 CONCLUSIONS

We have calculated the rates of disruption of stars by central BHs in two-integral models of nearby galaxies. Our simplest calculation (Section 3) is based on the assumption that all stars are on centrophobic loop orbits. Then there is a small portion of phase space, the loss cone $J < J_{\rm lc}$, within which stars will be consumed by the BH within an orbital period. Two-body relaxation causes stars to diffuse into this loss cone, but at a very low rate: only for loosely bound orbits in the faintest, most compact galaxies is the diffusion strong enough to keep the loss cone full.

Real galaxies are not, however, composed entirely of stars on loop orbits. In the presence of the slightest degree of flattening, a significant portion of phase space is occupied by centrophilic orbits, so that the loss cone becomes a 'loss wedge' (Section 4). In a steady state, this loss wedge feeds stars to the BH at a rate that is almost always faster than would be obtained if all stars were on centrophilic loop orbits; however, the enhancement is typically less than a factor of 2 or so. There is nevertheless one important difference in the nature of the disruption in the two cases: stars on centrophobic orbits are more likely to approach the BH on deeply plunging radial orbits, with pericentres well within $r_{\rm t}$. Stars on these ultraclose orbits are expected to 'pancake', possibly with an explosive release of energy (e.g. Carter & Luminet 1982; Rees 1988, 1998).

The best places to look for evidence of tidal disruption are faint ($L_V \lesssim 10^{10}\,\mathrm{L}_\odot$) bulges with steep, power-law central density cusps. In such galaxies, two-body relaxation causes a main-sequence star to wander into the maw of the BH every 10^4 to 10^5 yr, yielding a visible flare. Surveys sensitive to flares out to a redshift $z = 0.3$ (e.g. current R-band supernovae searches) are expected to see only about one flare per $10\,\mathrm{deg}^2$ per yr. It might be possible that V-band surveys could yield much higher rates. Apart from the extra complications introduced by centrophilic orbits mentioned above, our results are in broad agreement with those of Syer & Ulmer (1999).

Flares occur much less frequently in larger galaxies (assuming that their DFs are roughly isotropic), partly because such galaxies have BHs with $M_\bullet \gtrsim 10^8\,\mathrm{M}_\odot$ that swallow main-sequence stars whole, and partly because such galaxies are less centrally concentrated, meaning that their time-scales are much longer. The flaring rate from the two-body relaxation of giants into the loss cone of a large galaxy can be as low as $10^{-9}\,\mathrm{yr}^{-1}$. On the other hand, the slow time-scales mean that the depletion of the stock of stars on centrophilic orbits occurs much more slowly than in compact power-law galaxies. We estimate that the disruption of giant stars on low-J centrophilic orbits could occur as often as once every 10^5 yr or so in the largest galaxies. However, very large galaxies are extremely rare, and so will not affect the expected detection rate in surveys. This enhanced rate of fuelling from centrophilic orbits is also important in other contexts (e.g. hardening of black-hole binaries – Begelman, Blandford & Rees 1980; generation of gravitational waves from stellar remnants passing close to the BH – Sigurdsson & Rees 1997).

At least two processes might change the flaring rate dramatically, neither of which unfortunately is easy to model. First, the BH may wander from the centre of mass of the galaxy. Secondly, a modest degree of radial anisotropy could increase the flaring rate dramatically, although this enhancement is very sensitive to the observationally inaccessible details of the DF for near-radial orbits.

ACKNOWLEDGMENTS

We thank David Merritt, Saul Perlmutter, Martin Rees, Dave Syer and our collaborators on the Nuker team for useful conversations and correspondence. Financial support to JM was provided by NSERC and PPARC. Partial support for this work was provided by NASA through grant number NAG5-7066, and grant GO-07388.06-96A from the Space Telescope Science Institute, which is operated by the Association of Universities for Research in Astronomy, Inc., under NASA contract NAS5-26555.

REFERENCES

Bahcall J. N., Wolf R. A., 1976, ApJ, 209, 214
Begelman M. C., Blandford R. D., Rees M. J., 1980, Nat, 287, 307
Beloborodov A. M., Illarionov A. F., Ivanov P. B., Polnarev A. G., 1992, MNRAS, 259, 209
Binggeli B., Sandage A., Tammann G. A., 1988, ARA&A, 26, 509
Binney J., Tremaine S., 1987, Galactic Dynamics, Princeton University Press, Princeton
Binney J., Lacey C., 1988, MNRAS, 230, 597
Carter B., Luminet J. P., 1982, Nat, 296, 211
Chokshi A., Turner E. L., 1992, MNRAS, 259, 421
Cohn H., Kulsrud R. M., 1978, ApJ, 226, 1087 (CK)
Diener P., Kosovichev A. G., Kotok E. V., Novikov I. D., Pethick C. J., 1995, MNRAS, 275, 498
Efstathiou G., Ellis R. S., Peterson B. A., 1988, MNRAS, 232, 431
Faber S. M. et al., 1997, AJ, 114, 1771
Ferguson H. C., Sandage A., 1991, AJ, 101, 765
Ford H. C., Tsvetanov Z. I., Ferrarese L., Jaffe W., 1998, in Sofue Y., ed., Proc. IAU Symp. 184, The Central Regions of the Galaxy and Galaxies. Kluwer, Dordrecht, p. 377
Frank J., Rees M. J., 1976, MNRAS, 176, 633
Gerhard O. E., Binney J. J., 1985, MNRAS, 216, 467
Gerhard O. E., Jeske G., Saglia R. P., Bender R., 1998, MNRAS, 295, 197
Ho L. C., 1998, in Chakrabarti S. K., ed., Observational Evidence for Black Holes in the Universe. Kluwer, Dordrecht, p. 157
Jaffe W., 1983, MNRAS, 202, 995
Kippenhahn R., Weigert A., 1990, Stellar Structure and Evolution, Springer-Verlag, Berlin
Komossa S., Bade N., 1999, A&A, submitted (astro-ph/9901141)
Kormendy J., Richstone D., 1995, ARA&A, 33, 581
Landau L., 1937, Zh. Eksper. Theor. Fiz., 7, 203
Lauer T. R. et al., 1995, AJ, 110, 2622
Lauer T. R., Faber S. M., Ajhar E. A., Grillmair C. J., Scowen P. A., 1998, AJ, 116, 2263
Lee H. M., 1999, in Chakrabarti S. K., ed., Observational Evidence for Black Holes in the Universe. Kluwer, Dordrecht, p. 187
Lichtenberg A. J., Lieberman M. A., 1992, Regular and Chaotic Dynamics, 2nd edn. Springer-Verlag, New York
Lightman A. P., Shapiro S. L., 1977, ApJ, 211, 244
Lynden-Bell D., 1969, Nat, 223, 690
Magorrian S. J., 1999, MNRAS, 302, 530
Magorrian J. et al., 1998, AJ, 115, 2285 (Paper I)
Maoz E., 1998, ApJ, 494, L181
Merritt D., Oh S. P., 1997, AJ, 113, 1279
Merritt D., Quinlan G. D., 1998, ApJ, 498, 625
Miralda-Escudé J., Schwarzschild M., 1989, ApJ, 339, 752
Norman C., Silk J., 1983, ApJ, 266, 502
Novikov I. D., Pethick C. J., Polnarev A. G., 1992, MNRAS, 255, 276
Pain R. et al., 1996, ApJ, 473, 356
Press W. H., Flannery B. P., Teukolsky S. A., Vetterling W. T., 1992, Numerical Recipes in C, 2nd edn. Cambridge University Press, Cambridge
Rauch K., Ingalls B., 1998, MNRAS, 299, 1231

Rauch K., Tremaine S., 1996, New Astron., 1, 149
Rees M., 1988, Nat, 333, 523
Rees M., 1998, in Wald R., ed., Black Holes and Relativistic Stars. University of Chicago Press, Chicago, p. 79
Renzini A., Greggio L., di Serego Allghieri S., Cappellari M., Burstein D., Bertola F., 1995, Nat, 378, 39
Richstone D. et al., 1998, Nat, 395, A14
Rix H.-W., de Zeeuw P. T., Cretton N., van der Marel R. P., Carollo C. M., 1997, ApJ, 488, 702
Sandage A., Tammann G. A., Yahil A., 1979, ApJ, 232, 352
Schechter P., Dressler A., 1987, AJ, 94, 563
Sigurdsson S., Rees M. J., 1997, MNRAS, 284, 318
Sołtan A., 1982, MNRAS, 200, 115
Spitzer L., Hart M. H., 1971, ApJ, 164, 399
Sridhar S., Touma J., 1997, MNRAS, 287, L1
Sridhar S., Tremaine S., 1992, Icarus, 95, 86
Syer D., Ulmer A., 1999, MNRAS, 306, 35
Touma J., Tremaine S., 1997, MNRAS, 292, 905
Tremaine S., 1995, AJ, 110, 628
Ulmer A., 1999, ApJ, 514, 180
Ulmer A., Paczyński B., Goodman J., 1998, A&A, 333, 379
van der Marel R. P., 1998, in Saunders D. B., Barnes J., eds, Proc. IAU Symp. 186, Galaxy Interactions at Low and High Redshift. Kluwer, Dordrecht, p. 333
Weinberg M. D., 1994, ApJ, 421, 481
Yahil A., Sandage A., Tammann G. A., 1980, ApJ, 242, 448
Young P. J., 1977, ApJ, 212, 227

APPENDIX A: GENERALIZATION TO A SPECTRUM OF STELLAR MASSES

A1 Main-sequence stars

It is straightforward to generalize the calculations in the body of this paper to a range of stellar masses and radii. Let us assume that the probability of finding a main-sequence star with mass in the range m_* to $m_* + \mathrm{d}m_*$ within some phase-space volume $\mathrm{d}^3\boldsymbol{x}\,\mathrm{d}^3\boldsymbol{v}$ around $(\boldsymbol{x},\boldsymbol{v})$ is

$$f(\boldsymbol{x},\boldsymbol{v};m_*)\,\mathrm{d}^3\boldsymbol{x}\,\mathrm{d}^3\boldsymbol{v}\,\mathrm{d}m_* = f_\odot(\boldsymbol{x},\boldsymbol{v})n(m_*)\,\mathrm{d}^3\boldsymbol{x}\,\mathrm{d}^3\boldsymbol{v}\,\mathrm{d}m_*, \tag{A1}$$

with

$$n(m_*) = \begin{cases} A(m_*/\mathrm{M}_\odot)^{-x}, & m_1 < m_* < m_2 \\ 0 & \text{otherwise,} \end{cases} \tag{A2}$$

and $f_\odot$ the DF obtained by inverting equation (7) assuming the galaxy is composed of solar-type stars. We take $m_1 = 0.08\,\mathrm{M}_\odot$, $m_2 = 1\,\mathrm{M}_\odot$ (no recent star formation) and $x = 2.35$ (Salpeter mass function). This DF has to reproduce the mass distribution and mass-to-light ratio inferred from observations, so that (see also equation 7)

$$\rho(0,z) = 4\pi\int_0^{\psi(0,z)} f_\odot(\mathscr{E},0)\sqrt{2[\psi(0,z)-\mathscr{E}]}\,\mathrm{d}\mathscr{E} \times \int_{m_1}^{m_2} m_* n(m_*)\,\mathrm{d}m_*. \tag{A3}$$

Therefore $\int_{m_1}^{m_2} m_* n(m_*)\,\mathrm{d}m_* = \mathrm{M}_\odot$ so that

$$A = \frac{2-x}{\mathrm{M}_\odot}\left[\left(\frac{m_2}{\mathrm{M}_\odot}\right)^{2-x} - \left(\frac{m_1}{\mathrm{M}_\odot}\right)^{2-x}\right]^{-1} = 0.246\,\mathrm{M}_\odot^{-1}. \tag{A4}$$

For lower main-sequence stars, $r_* \sim m_*^{0.8}$ (Kippenhahn & Weigert 1990). So from equation (1), the tidal disruption radius $r_\mathrm{t} \propto m_*^{0.467}$. A main-sequence star, the mass of which satisfies

$$m_* < m_{\min}(M_\bullet) \equiv a\left(\frac{M_\bullet}{10^8\,\mathrm{M}_\odot}\right)^{1.43}\mathrm{M}_\odot, \tag{A5}$$

will be swallowed whole by the BH; here a is a constant of order unity (= 1.05 for $n = 3$ polytropes; see Diener et al. 1995).

From Appendix B, the diffusion coefficient for two-body relaxation

$$\mu_{\mathrm{MF}} = \mu_\odot\int_{m_1}^{m_2}\left(\frac{m_*}{\mathrm{M}_\odot}\right)^2 n(m_*)\,\mathrm{d}m_* \simeq 0.31\mu_\odot. \tag{A6}$$

If we ignore the $\ln R_0$ factor in equation (23), two-body relaxation gives a flaring rate

$$F^{\mathrm{lc}}_{\mathrm{MF}}(\mathscr{E}) = F^{\mathrm{lc}}_\odot(\mathscr{E})\frac{\mu_{\mathrm{MF}}}{\mu_\odot}\int_{\max[m_1,m_{\min}(M_\bullet)]}^{m_2} n(m_*)\,\mathrm{d}m_*, \tag{A7}$$

which for $M_\bullet < 1.7\times10^7\,\mathrm{M}_\odot$ is $1.66F^{\mathrm{lc}}_\odot$. In calculating the $F^{\mathrm{lc}}_{\mathrm{MF}}$ reported in Table 1, we have taken into account the $\ln R_0$ factor in equation (23), giving slightly higher results than this. The effects of the mass spectrum on the F^{lw} given by equation (49), and on the F^{drain} given by equations (41) and (44), are dealt with in a similar way.

A2 Giant stars

A small fraction $g \ll 1$ of stars will be giants with some characteristic radius r_g. These are the only stars that produce flares in large galaxies with $M_\bullet > 10^8\,\mathrm{M}_\odot$. We take $g = 0.01$ and $r_\mathrm{g} = 15\mathrm{r}_\odot$. From equations (23) and (49), giants contribute a factor $g(\mu_{\mathrm{MF}}/\mu_\odot)$ times $F^{\mathrm{lc}}_\odot$ or $F^{\mathrm{lw}}_\odot$ to the rates in the diffusion limit, rising to a factor $g(r_\mathrm{g}/\mathrm{r}_\odot)(\mu_{\mathrm{MF}}/\mu_\odot)$ in the pinhole limit. It is straightforward to calculate their contribution to $F^{\mathrm{drain}}_{\mathrm{MF}}$ using equations (41) and (44).

Finally, there is a further way of feeding giant stars to the BH. In the normal course of stellar evolution, a main-sequence star on a low-angular-momentum orbit may turn into a giant and suddenly find itself in the wider, giant loss cone (Syer & Ulmer 1999). We ignore this process, as it has negligible effect compared with, for example, the draining of giant stars on the loss wedge (Section 4.1.1).

APPENDIX B: DIFFUSION COEFFICIENTS

In this Appendix we derive expressions for the diffusion coefficients used in equation (17) in the limit $R \to 0$. Because of the presence of the loss cone, the steady-state distribution of scatterers is not quite isotropic. It is, however, reasonable to calculate the diffusion coefficients using the isotropized distribution function

$$\bar{f}(\mathscr{E}) \equiv \int_0^1 f(\mathscr{E},R)\,\mathrm{d}R. \tag{B1}$$

We make the reasonable approximation that all encounters take place instantaneously and so change the velocity of the scattered star but not its position. In addition, we make the usual (although more dubious) assumption that the distribution of scatterers is homogeneous in space. Since $R \equiv r^2v_\mathrm{t}^2/J_\mathrm{c}^2(\mathscr{E})$, where $v_\mathrm{t}^2 = v_\phi^2 + v_\theta^2$, we can immediately use equation (8-64) of Binney & Tremaine (1987) to show that

$$\langle\Delta R\rangle = \frac{32\pi^2r^2G^2m_*^2\ln\Lambda}{3J_\mathrm{c}^2}(3I_{\frac{1}{2}} - I_{\frac{3}{2}} + 2I_0) + \mathscr{O}(R), \tag{B2}$$

where

$$I_0 \equiv \int_0^{\mathscr{E}} \bar{f}(\mathscr{E}')\,\mathrm{d}\mathscr{E}',$$
$$I_{\frac{n}{2}} \equiv [2(\psi(r)-\mathscr{E})]^{-\frac{n}{2}} \int_{\mathscr{E}}^{\psi(r)} [2(\psi(r)-\mathscr{E}')]^{\frac{n}{2}} \bar{f}(\mathscr{E}')\,\mathrm{d}\mathscr{E}', \tag{B3}$$

and $\ln\Lambda$ is the usual Coloumb logarithm. We follow Spitzer & Hart (1971) and take $\Lambda = 0.4M_\bullet/m_*$.

The second-order diffusion coefficient is $\langle(\Delta R)^2\rangle = r^4(\Delta v_\mathrm{t}^2)^2/J_\mathrm{c}^4(\mathscr{E})$. Since

$$(\Delta v_\mathrm{t}^2)^2 = 4v_\theta^2(\Delta v_\theta)^2 + 4v_\phi^2(\Delta v_\phi)^2 + 8v_\theta v_\phi \Delta v_\theta \Delta v_\phi + \mathscr{O}[(\Delta v)^3], \tag{B4}$$

it follows from equations (8-64) and (8-65) of Binney & Tremaine (1987) that

$$\langle(\Delta R)^2\rangle = R\frac{64\pi^2 r^2 G^2 m_*^2 \ln\Lambda}{3J_\mathrm{c}^2}(3I_{\frac{1}{2}} - I_{\frac{3}{2}} + 2I_0) + \mathscr{O}(R^2). \tag{B5}$$

Notice that $\langle\Delta R\rangle = \frac{1}{2}\partial\langle(\Delta R)^2\rangle/\partial R$, the orbit-averaged version of which holds generally whenever the scattering is done by an external perturbation (Landau 1937; Binney & Lacey 1988).

APPENDIX C: NUMERICAL SOLUTION FOR THE DISTRIBUTION FUNCTION

For each galaxy model, we need to find a smooth DF $f(\mathscr{E})$ that provides an acceptable fit to the number-density profile $\nu(r)$ and potential $\psi(r)$ of the model through

$$\nu(r) = 4\pi\int_0^{\psi(r)} f(\mathscr{E})\sqrt{2[\psi(r)-\mathscr{E}]}\,\mathrm{d}\mathscr{E}. \tag{C1}$$

The number density is given on a grid $(\log r_i, \log\nu(r_i))$ with $n_\nu \sim 60$ points, equispaced in $\log r$. We represent $f(\mathscr{E})$ on a grid $(\log r(\mathscr{E}_i), \log f(\mathscr{E}_i))$ with $r(\mathscr{E})$ defined such that $\mathscr{E} = \psi(r(\mathscr{E}))$. This grid has $n_f = 1.5n_\nu$ points, with r running logarithmically from the radius of the innermost $\nu(r)$ point to a few times the radius of the outermost one. Values of $f(\mathscr{E})$ at intermediate points are obtained by linear interpolation in $(\log r(\mathscr{E}), \log f(\mathscr{E}))$.

For a given trial $f(\mathscr{E})$, it is straightforward to integrate equation (C1) numerically to obtain the density distribution $\bar{\nu}(r)$ of that model. We measure the goodness of fit of each model using

$$\chi^2 \equiv \sum_{i=1}^{n_\nu}\left(\frac{\nu_i - \bar{\nu}_i}{\nu_i}\right)^2. \tag{C2}$$

Not all trial DFs that produce a low χ^2 are equally acceptable though, because some will be more jagged than others. We penalize jagged solutions using a penalty function that measures the mean-square change in $\mathrm{d}f(\mathscr{E})/\mathrm{d}r(\mathscr{E})$:

$$P[f] \equiv \frac{1}{n_f}\sum_{i=2}^{n_f-1}\left(\frac{\log f(\mathscr{E}_{i+1}) - 2\log f(\mathscr{E}_i) + \log f(\mathscr{E}_{i-1})}{\Delta\log r(\mathscr{E})}\right)^2. \tag{C3}$$

Then our most acceptable model is the one that maximizes the penalized likelihood $\mathscr{L}$ defined through

$$\log\mathscr{L} \equiv -\frac{1}{2}\chi^2 - \lambda P[f]. \tag{C4}$$

We somewhat arbitrarily choose λ such that a change in $P[f]$ of 10 causes the same change in $\mathscr{L}$ as a change in χ^2 of $10^{-4}n_\nu$ (a change in the rms fractional error of 0.01). Choosing different values for λ causes insignificant changes in the resulting DF.

Our procedure for maximizing equation (C4) is as follows. First we fit an initial parametrized model of the form

$$f(\mathscr{E}) = A\left(\frac{r(\mathscr{E})}{r_0}\right)^\alpha\left(\frac{1+r(\mathscr{E})}{r_0}\right)^\beta \tag{C5}$$

to the given $\nu(r)$. We find the parameters (A, r_0, α, β) that minimize χ^2 using the downhill-simplex method (Press et al. 1992). Then we use the Metropolis algorithm in the form described by Magorrian (1999) to maximize $\mathscr{L}$. After a few thousand iterations of the Metropolis algorithm, the model is still acceptably smooth, with a typical rms fractional error in $\nu(r)$ of 0.01 or better.

This paper has been typeset from a TEX/LATEX file prepared by the author.